3. SITE 809[1]

Shipboard Scientific Party[2]

HOLE 809A

Date occupied: 13 June 1990

Date departed: 14 June 1990

Time on hole: 1 day, 6 hr, 15 min

Position: 31°03.439′N, 139°52.721′E

Bottom felt (rig floor; m; drill pipe measurements): 1830.8

Distance between rig floor and sea level (m): 11.1

Water depth (drill-pipe measurement from sea level, m): 1819.7

Total depth (rig floor; m): 1831.1

Penetration (m): 8.3

Number of cores (including cores with no recovery): none

Total length of cored section (m): 0

Total rock recovered (m): 0.01

Core recovery (%): n/a

Hard rock:
Depth sub-bottom (m): 8.3
Nature: vesicular basalt scoria

Comments: Recovery was bit sample

HOLE 809B

Date occupied: 14 June 1990

Date departed: 15 June 1990

Time on hole: 21 hr

Position: 31°03.48′N, 139°52.66′E

Bottom felt (rig floor; m; drill pipe measurements): 1810.7

Distance between rig floor and sea level (m): 11.1

Water depth (drill pipe measurement from sea level, m): 1799.6

Total depth (rig floor; m): 1824.1

Penetration (m): 13.4

Number of cores (including cores with no recovery): 0

Total length of cored section (m): 0

Total core recovered (m): 0

HOLE 809C

Date occupied: 15 June 1990

Date departed: 24 June 1990

Time on hole: 8 days, 17 hr, 45 min

Position: 31°03.50′N, 139°52.63′E

Bottom felt (rig floor; m; drill pipe measurements): 1812.6

Distance between rig floor and sea level (m): 11.1

Water depth (drill pipe measurement from sea level, m): 1801.5

Total depth (rig floor; m): 1816.7

Penetration (m): 4.1

Number of cores (including cores with no recovery): 0

Total length of cored section (m): 0

Total core recovered (m): 0

HOLE 809D

Date occupied: 24 June 1990

Date departed: 27 June 1990

Time on hole: 3 days, 10 hr, 45 min

Position: 31°03.49′N, 139°52.67′E

Bottom felt (rig floor; m; drill pipe measurements): 1813.0

Distance between rig floor and sea level (m): 11.1

Water depth (drill pipe measurement from sea level, m): 1802.0

Total depth (rig floor; m): 1819.3

Penetration (m): 6.3

Number of cores (including cores with no recovery): 0

Total length of cored section (m): 0

Total core recovered (m): 0

HOLE 809E

Date occupied: 27 June 1990

Date departed: 29 June 1990

Time on hole: 4 days, 13 hr, 15 min

Position: 31°03.51′N, 139°52.64′E

Bottom felt (rig floor; m; drill pipe measurements): 1814.1

Distance between rig floor and sea level (m): 11.1

Water depth (drill pipe measurement from sea level, m): 1803.0

Total depth (rig floor; m): 1822.1

Penetration (m): 8.0

Number of cores (including cores with no recovery): 0

Total length of cored section (m): 0

Total core recovered (m): 0

HOLE 809F

Date occupied: 29 June 1990

Date departed: 18 July 1990

Time on hole: 19 days, 15 hr

Position: 31°03.50′N, 139°52.64′E

Bottom felt (rig floor; m; drill pipe measurements): 1813.6

Distance between rig floor and sea level (m): 11.1

Water depth (drill pipe measurement from sea level, m): 1802.5

Total depth (rig floor; m): 1892.8

Penetration (m): 79.2

1 Storms, M. A., Natland, J. H., et al., 1991. *Proc. ODP, Init. Repts.*, 132: College Station, TX (Ocean Drilling Program).

2 Shipboard Scientific Party is as given in the list of participants preceding the contents.

Number of cores (including cores with no recovery): 34

Total length of cored section (m): 59.00

Total core recovered (m): 11.13

Core recovery (%): 18.70

Hard rock:

Depth sub-bottom (m): 79.20
Nature: fine grained vesicular basalt
Measured velocity (km/s):

Comments: Drill-in BHA 5.9 m; drilled with DCS 14.3 m. Core 132-809F-34B was a bit core from previously cored interval 78.6–79.2 mbsf.

13 June–25 June 1990: Initial Hard Rock Base Installation

During the approach to Site 809, we passed from north to south over the crest of a line of small volcanic ridges to locate ourselves precisely within the HIG Seabeam bathymetric survey. The site was chosen to be as close as possible to the crest of the ridge at a saddle between two of the small peaks, this area appearing to offer the flattest seafloor for setting of a guide base. The crest line at the low point of the saddle was precisely located on an east to west pass, and the beacon was dropped there on the return pass. Currents carried the beacon about 150 m to the southeast before it reached the seafloor.

Two short surveys of the seafloor were carried out using a Mesotech acoustic scanner and TV camera, one before each of the first two holes we drilled. The seafloor consists of slightly sedimented scoriaceous pillow lava, with pillow diameters ranging from less than 0.5 m to more than 2 m. The beacon itself was located near a 10 m high flow front, but the flow is fairly flat upslope to the west. Here, 30 m south and 34 m west of the beacon, we spudded our first hole, Hole 809A, which was drilled using the positive-displacement coring motor to test the capability of a newly-designed 11-5/8 in. bit/center-bit assembly in coring volcanic rock. Using the coring motor, and 2000–5000 lbs weight on bit, the hole reached 8.3 m in 7 hr, a rate of 1.2 m/hr. No cores were taken. Wear on the bit was negligible. The TV monitor revealed a crater about 2 m in diameter around the pipe, indicating that caving had occurred around the top of the hole. The caving was probably aggravated by the "whipping" action of the coring motor during the unsupported spudding operation.

The next test hole, Hole 809B, was drilled in the same manner with a smaller newly-designed bit 9-7/8 in. in diameter, again with a center bit. The hole was about 100 m farther to the northwest, on a similar but probably somewhat older flow of pillow lavas, with ponded sediment between the pillows. Here, closer to the presumed rift axis, we hoped for smoother drilling conditions and even less basement relief. The bit indeed produced a narrower hole (<1 m diameter) with less caving, and reached 13.4 m in 8.3 hr, a rate of 1.6 m/hr. Again, bit wear was negligible. Using the Mesotech acoustic scanner, we identified a particularly flat area away from local flow fronts or pillow ridges that produced backscatter shadows of 2–3 m at distances of 20–30 m on the display. The coordinates of the flat patch relative to the beacon were noted for reference during the guide-base operation. This was fortunate because the Mesotech scanning sonar failed during the guide-base lowering and did not function thereafter.

The guide base, which during this time was being constructed over the moon pool, was lowered to start Hole 809C, and reached the seafloor at 1100 hr on 16 June. Setting the base on the seafloor was done blindly, since the VIT frame holding the TV camera was unable to see below the guide base to view the bottom. With the weight of the base released from the drill string, we disconnected the pipe by rotating the jay-tool and backing out of the cone. To our great surprise, the cone quickly lurched away from the camera to one side, and then leaned into one corner of the central cavity within the hard rock base. Initially, we feared that the basement surface was too steep, but examination of video tapes and subsequent operations established instead that the problem was insufficient syntactic foam to provide buoyancy to right the cone to the vertical above its gimbal assembly. With the jay-tool still down, we did a test reentry, and used the weight of the drill string plus the ship's dynamic positioning system to pull the cone upright.

With some reentry capability established, we retrieved the pipe and ran in with a core bit and drill-in BHA. The design was intended to case off about 6 m of hole and thus provide sidewall stability at the outset of diamond coring operations, and simultaneously to lock the cone into a vertical position. After drilling 6 m, the pipe was to separate automatically from the BHA by means of a tapered back-off sub, leaving the lower portion of the BHA in the hole and below the jay-slot. Unfortunately, the back-off sub rotated free after only 4.1 m of penetration at Hole 809C, leaving the top of the casing above the bottom of the jay-slot. This was confirmed during our next reentry with the jay-tool.

We tripped the pipe and sent down a tool to fish the BHA. The reentry and fishing operation went smoothly, but the cone — freed of the supporting casing — once again fell to the south corner of the weighted base. We elected this time to drill a "rat-hole" into which the same back-off system could simply be lowered without fear of premature operation of the back-off sub. However, on this reentry attempt, we had great difficulty in pulling the cone upright. We managed to get into the throat of the cone, but at an angle that did not allow the bottom-hole assembly to pass through the casing hanger to the seafloor. Reentry in this circumstance requires pivoting the cone to a nearly upright position, and then working the bit into the casing hanger. Alternatively, the string can be slid down one side of the inclined cone at an angle (produced by draping the pipe into the cone by means of offsetting the ship). Hopefully the angle can come close to that of the gimbaled casing hanger. The risk is that such operations can produce strong excursions of the cone about the pipe as it rotates about its gimbal assembly. The situation was exacerbated by rocking of the weighted base itself on two legs as the cone swung and lurched into the sides of the box. This is because the four-legged base can only sit on three legs on an irregular basement surface. Bit weight on the sides of the cone applies moments to either side of the base which is centered on a line between the two stable legs. Thus, it must wobble.

During one such pirouette on this reentry attempt, the cone swung out of a pinned position, and the drill string itself fell away, imparting a sharp lateral blow to the inner lower surface of the cone. This caused the cone to separate partially from its welded base and gusset support assembly where it joined the casing hanger. The cone could not safely be reentered in this condition, so we elected to push it completely off the casing hanger using the drill string. The cone fell to the seafloor upside down, confirming that the flotation was inadequate to support the cone even without that portion of the casing hanger above the gimbal.

The casing hanger itself, however, offered a small, 24 in. diameter opening through which reentries might be accomplished. The hanger would still have to be pulled to an upright position, but there was no reason why we should not attempt it.

Regrettably, although we were able to put the end of the string into this tiny opening several times, and with more than one configuration of a bottom-hole assembly during two additional pipe trips, we never succeeded again in getting the drill-in BHA past the jay-tool assembly. Almost certainly, this was because we

could not hold the end of the string in the top of the hanger and relieve enough weight to drag it into a vertical position. The rocking hard rock base complicated these attempts.

At this point, our discussions turned to abandoning this guide base and setting the other one on board onto the seafloor. The flotation problem still existed, however. The only way to solve it was to retrieve the inverted cone with its flotation foam from the seafloor and use it together with the foam for the second guide base, all on one assembly. A fishing tool with four arms arranged like a molly-bolt was lowered to the seafloor and speared through the inverted opening at the cone's base. The simple tool worked well, and the cone was back on deck within a few hours.

Emboldened by this success, we decided to fish for the guide base. If this could be retrieved, then we would not lose the site planned for the second guide base later in the leg. A double jay tool was lowered on flexible 5 in. drill pipe. No other BHA components were used. The hard rock base was located with the TV, and the 24 in. opening in the casing hanger reentered. The hanger was pulled from the south to the north corner of the base by offsetting the ship to allow a maximum alignment of the flexible pipe with the tilted end of the hanger. After rotating the jay-tool with the coring motor, we finally found an orientation which allowed it to slip into the jay-assembly. Another partial turn engaged the tool, and we lifted the guide base from the seafloor to the moon pool.

Once on deck, the reincarnated guide base was then refitted by lightening the cone, doubling up the foam, and reattaching the cone to its base. We constructed a tilt beacon to be assured that the base would rest on sufficiently flat bottom, and added markings and inclinometers to the base to determine its orientation after we disconnected from the cone. This completed, the base with its cone was returned to the depths and landed. The base on the new hole (809D), had a 15° slope on a pillowed surface, and the cone floated freely from its gimbal above it.

June 25–July 18, 1990: Hard Rock Base Maneuvering and Coring with the Diamond Coring System

After lowering the reconstructed guide base, several additional difficulties with the seafloor installation had to be overcome before we established a workable hole at Site 809. At Hole 809D, although we succeeded in emplacing the drill-in BHA in the casing hanger and stabilizing the reentry cone, a failure of the jay-tool left a 6 in. slab of metal in the throat of the guide base. The damaged tool was retrieved and the remaining tool on board strengthened. This was then tripped back down to the cone, jayed-in, and then used to lift the base over the drill-in casing, leaving the casing embedded in the seafloor. We moved the hard rock base a few meters to Hole 809E. Using the TV monitor, the metal slab was seen resting on the top of the drill-in BHA after we lifted the base.

At Hole 809E, after some hours attempting to drill in another BHA, we managed to erode and undercut the basalt underlying one leg of the hard rock base, causing it to tilt beyond the 20° maximum allowed by the reentry-cone gimbal assembly. We retrieved the casing, tripped back to the cone, jayed-in, and once again moved the base across the seafloor to a new location, Hole 809F, where finally we succeeded in drilling in and latching a BHA to a depth of 5.9 m below the seafloor (mbsf).

There followed a period of assembly and testing of the DCS. Several problems were discovered with the secondary heave compensation system, most of them having to do with noise imparted to controlling accelerometers mounted on the DCS platform. The most serious complications were resonance sent down the pipe (which was held in tension against the weight of the hard rock base) and returned to the ship, and noise from the DCS platform's hydraulic feed cylinders. Both would change — sometimes hourly — as sea-state, wind, and ship's orientation changed. Eventually, the problem was overcome by shifting the sensor system to the ship's hull in the moon pool, thereby bypassing the fluctuating, high-frequency motions of the platform and hydraulic system. For most of the time we were coring, however, the full heave compensation system was not in use.

Coring with the DCS began on 6 July. Adjustments had to be made to input parameters in the controlling computer program, inasmuch as changes in weight-on-bit caused simply by landing the bit on the bottom of the hole were initially interpreted by the computer as breakthroughs in the formation ("void hits"). This triggered automatic pull-backs of the drill string. Also, about 2 m below the bottom of the casing, we encountered what we interpret as a flow-top breccia which was extremely quickly drilled, and which took almost no weight on bit. Virtually none of this material was recovered, evidently because it was either washed out ahead of the bit by down-the-pipe circulating fluids, or because it fell out of the core barrels as they were retrieved. Throughout this time, there were several indications of possible core jams, based on pressure readings of the fluid pumped down the tubing. At least one such reading may have been caused by aggregation of lumps of gel separated from the lubricant added to the drilling fluid. Also, some core barrels may not have latched in because of accumulated debris (lost core) lodged above the bit. We finally concluded that our core barrels indeed were functioning properly, but that the formation itself was too friable to be cored and retained.

We proceeded with coring, now in harder formation, but soon were unable to advance because of bit failure at 14.3 mbsf. We tripped the tubing, unjayed the drill string, suspended the string in the derrick, set back the DCS platform, and tripped the DCS tubing for a bit change. Reversing this sequence, we resumed drilling.

With this second bit, we advanced through several highly vesicular basalt flows or pillows, with substantial recovery (64%) to a depth of 29 mbsf. Coring was fairly smooth and rapid.

Below this, however, we again encountered unconsolidated formation, and here we faced the most significant weakness of the coring system. For nearly 50 m of subsequent penetration, we recovered virtually nothing. Two or three small chips of basalt would occasionally arrive on deck, but otherwise all we could discover about the formation was based on particles of sand twice found in returned core barrels, and once on the chiseled face of a bit deplugger. The sand suggests the presence of crystal-vitric tuffs, but the small particle size is probably a consequence of drilling. The rate of advance was rapid; at times, there were abrupt drop-throughs of up to 1 m, possibly representing voids in the formation. For most of this interval, weight-on-bit was low and impossible to sustain for much distance. We reduced circulation to a bare minimum (at one point to nearly half the minimum recommended by the bit manufacturer) and devised traps to place in the plastic core liners in an attempt to recover anything at all. But no amount of coaxing could be used, no trick devised, to persuade material even to enter the core barrels. At one point, we lowered a center bit and, after drilling ahead for some meters, recovered it without so much as a scratch on its painted surface.

To the limited degree that we understand it, the problem is a combination of the design of the core catcher, the bit chosen for the coring, and the unconsolidated nature of the formation. First, the core catcher is designed to capture fractured but competent rock recovered at full-round core diameter. It has a wide throat. We had no expectation that unconsolidated breccias of such thickness would be at this location, thus we had no core catcher on board with fingers to capture gravel-sized or smaller rock fragments.

Secondly, we continuously pumped a viscous fluid combining seawater, weighted mud, and lubricant down the pipe while coring. This mixture passed through a narrow annulus at the base of the seated core barrel between it and the inner wall of the bit. The force of the spray was directed at the formation immediately ahead (1.5 cm) of the core barrel, evidently jetting the unconsolidated material away. This explains why not even the paint was removed from the center bit when it occupied the place of the core barrel.

Nonetheless, we eventually worked our way into more massive basalt flows once again, recovering a few fully cored pieces before the second bit wore out at 79.2 mbsf. Probably, bit wear was accelerated or caused by a sand-blasting effect in the long interval of unconsolidated material we had just penetrated.

At this point, we set back the DCS platform, and rigged for logging through the DCS tubing. The slim-line combined caliper and gamma tool went down the tubing, but did not pass an obstruction at the bit. The obstruction could not be cleared with the bit deplugger, so we retrieved the tubing to find 34 cm of basalt tightly wedged just above the throat of the bit. Sandy particles coated some of the rocks. Once again, we lowered the logging tool, this time through the drill pipe, but now we encountered another obstruction 2.3 m below the drill-in bottom-hole assembly. With the logging tool, we worked this down to 13.7 mbsf, but no further. As we no longer had the tubing string in place to drill out the obstruction, we elected to abandon the site after 1 month and 5 days of operations, leaving for Shatsky Rise (Site 810).

Site 809 Scientific Summary

In Hole 809F, three chemically distinct basalt types were encountered in the 73.3 m of igneous formation penetrated by the diamond coring system below the casing shoe at 5.9 m below the seafloor. Successively these are (1) fairly strongly fractionated ferrobasalt (Mg# = 0.43) from 5.9 to 21 mbsf; (2) moderately fractionated olivine tholeiite (Mg# = 0. 60) from 21 to 29 mbsf, just above the 50 m interval with very low recovery; and (3) another moderately fractionated olivine tholeiite (Mg# = 0.60) from just below this interval in the last core obtained, between 78.9 and 79.2 mbsf.

The basalts are all extremely sparsely phyric, highly vesicular tholeiites similar to basalts dredged, drilled, and sampled by submersible vessels from this incipient back-arc rift. They are pillows or thin flows with glassy exteriors and more crystalline interiors. All the rocks are extremely fresh, with only minor oxidative alteration evident near some fractures. Most vesicles are partially lined with unaltered glass; only a few are lined with pale green clays or iron oxyhydroxides. The vesicles are a very prominent feature of these basalts. All the rocks contain myriad irregular to round pinhole vesicles, but there are some very large vesicles (to 1 cm diameter) especially in the more evolved upper ferrobasalt. In this basalt, some of the larger vesicles are arrayed in trains across the rock face within pillow or flow interiors. Many of the larger vesicles are segregation vesicles, being partly filled with frozen melt, itself vesicular, which leaked into them as their walls ruptured during crystallization of the rock. One rock contains a fracture into which melt also leaked, annealing it completely. There is a good correlation between physical properties (velocity, density) and vesicle distribution in the basalts.

The basalts are glassy to spherulitic near quench margins, and more crystalline in the pillow/flow interiors. The less fractionated basalts carry minor olivine (no spinel) and have less abundant titanomagnetite than the ferrobasalt. There are a few rare plagioclase phenocrysts. Apart from the olivine, the crystallization sequence in all the basalts was the same: co-precipitating plagioclase and clinopyroxene were followed in intergranular spaces by spectacularly skeletal titanomagnetite and rare, tiny rods of ilmenite. Even tinier pyrrhotite spherules decorate the rims of the oxide minerals, thus segregated only during the very final stages of crystallization of the basalts.

The uppermost ferrobasalt and immediately underlying olivine tholeiite have the typical elevated K_2O (0.60% and 0.32%, respectively), Rb (10 and 5 ppm), and Ba (61 and 45 ppm) abundances, and the relatively low TiO_2 (1.7% at Mg# = 0.43; 1.2% at Mg# = 0.60), Zr (72 and 56 ppm) and Y (27 and 19 ppm) of many back-arc-basin basalts. They are virtually identical to basalts previously sampled from this volcanic ridge. The lowermost basalt, obtained below the 50 m interval with virtually no recovery, is similar in most respects to the olivine basalt above the interval of low recovery, but it has somewhat lower K_2O (0.29%) and much lower Ba (19 ppm) contents. In these respects it resembles basalts from Site 791 drilled during Leg 126 which are interpreted to represent syn-rift basalts dating from the early stages of the opening of the Sumisu rift.

We speculate that the interval of very low recovery represents highly vesicular and expanded basaltic breccia similar to the basalt "mousse" recovered at Site 791. The rock compositions and stratigraphy suggest that we cored through a thin carapace of back-arc basalts into syn-rift volcanic rocks deposited on subsided prerift basement. This projects on seismic profiler records to a shallow elevation at this location.

BACKGROUND AND OBJECTIVES

The objective at Site 809 was to accomplish a full test of the diamond coring system (DCS), the new, smaller version of the hard rock base (HRB), and the new drill-in bottom-hole assembly (DI-BHA) at an unsedimented, active volcanic rift. The site was to simulate coring conditions expected in basalts at the axial rift of the East Pacific Rise, which has been a long-standing, high-priority drilling objective. Specific engineering objectives are outlined in Storms and Natland (this volume).

In the western Pacific, active spreading ridges occur in a number of back-arc basins. One such back-arc basin which fell close to the ship's track of *JOIDES Resolution* in the western Pacific is the Mariana Trough, which has been spreading for about 5.5 m.y. (Hussong and Uyeda, 1982). The best-studied portion of the spreading center there (at about 18°N) lies in about 3500 m of water.

To the north of the Mariana Trough and structurally homologous to it is an incipient rift west of the Bonin-Volcano and Izu arcs (Fig. 1). Regional and high-resolution bathymetric studies (Brown and Taylor, 1988; Taylor et al., in press) established the distribution of volcanoes and separate sedimented basins along this rift. One portion of the Bonin rift system, between 30°20′N and 31°20′N, is called the Sumisu Rift, after the nearest volcano in the Izu arc (Honza and Tamaki, 1985). Here, many dozens of small seafloor volcanoes are arrayed along northerly-trending fissures on a basement high at an accommodation zone separating the deeply sedimented North and South Sumisu Basins (Fig. 2). The largest coalesced grouping of these volcanoes straddles the narrowest portion of this basement high and is called Central Ridge. It consists of two en echelon rows of small volcanic peaks (Fig. 3). Camera tows, dredging, and submersible studies (Smith et al., in press; Fryer et al., in press; Hochstaedter et al., in press) show that Central Ridge is comprised primarily of pillow basalts with tholeiitic compositions fairly typical of back-arc spreading ridges. These rocks lie less than 20 km from active volcanoes of the Izu arc, and are quite distinct from basaltic/andesitic lavas found there. Central Ridge lies in only 1500–1900 m of water, thus was chosen in preference to the generally deeper Mariana Trough for DCS testing during Leg 132.

In order to approximate conditions at the East Pacific Rise most closely, a preliminary site was selected to sample basaltic

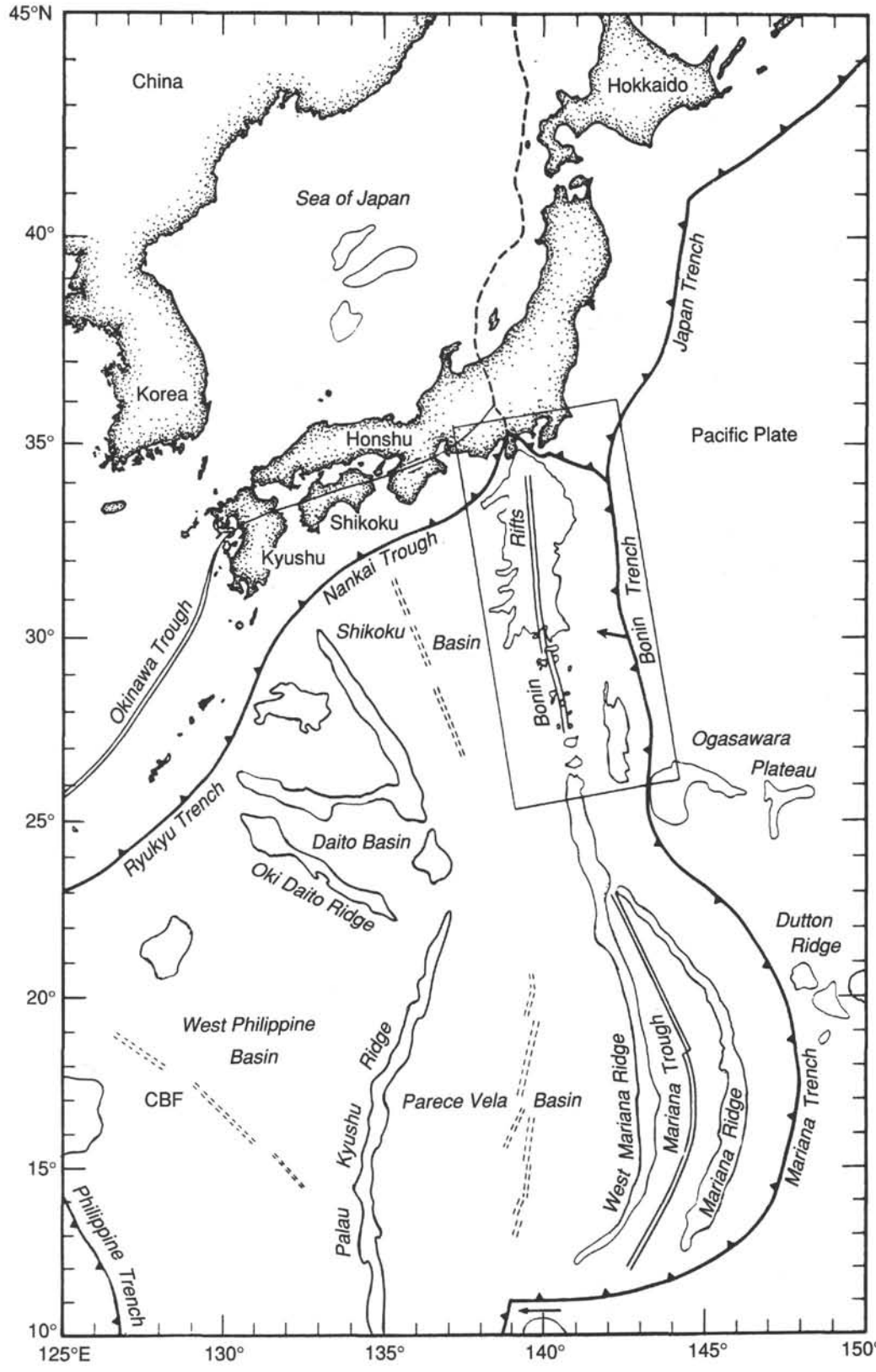

Figure 1. Bonin (Izu-Bonin, Izu-Ogasawara) arc (enclosed). Semi-isolated rifts have formed since the late Pliocene (Fujioka, Taylor, et al., 1989) between 27°N and 34°N (Taylor et al., in press). The arrow on the Bonin Trench is the direction of relative motion between the Pacific Plate and the Philippine Sea plate. Sumisu Rift is in the middle of the arc between 30°20′N and 31°30′N.

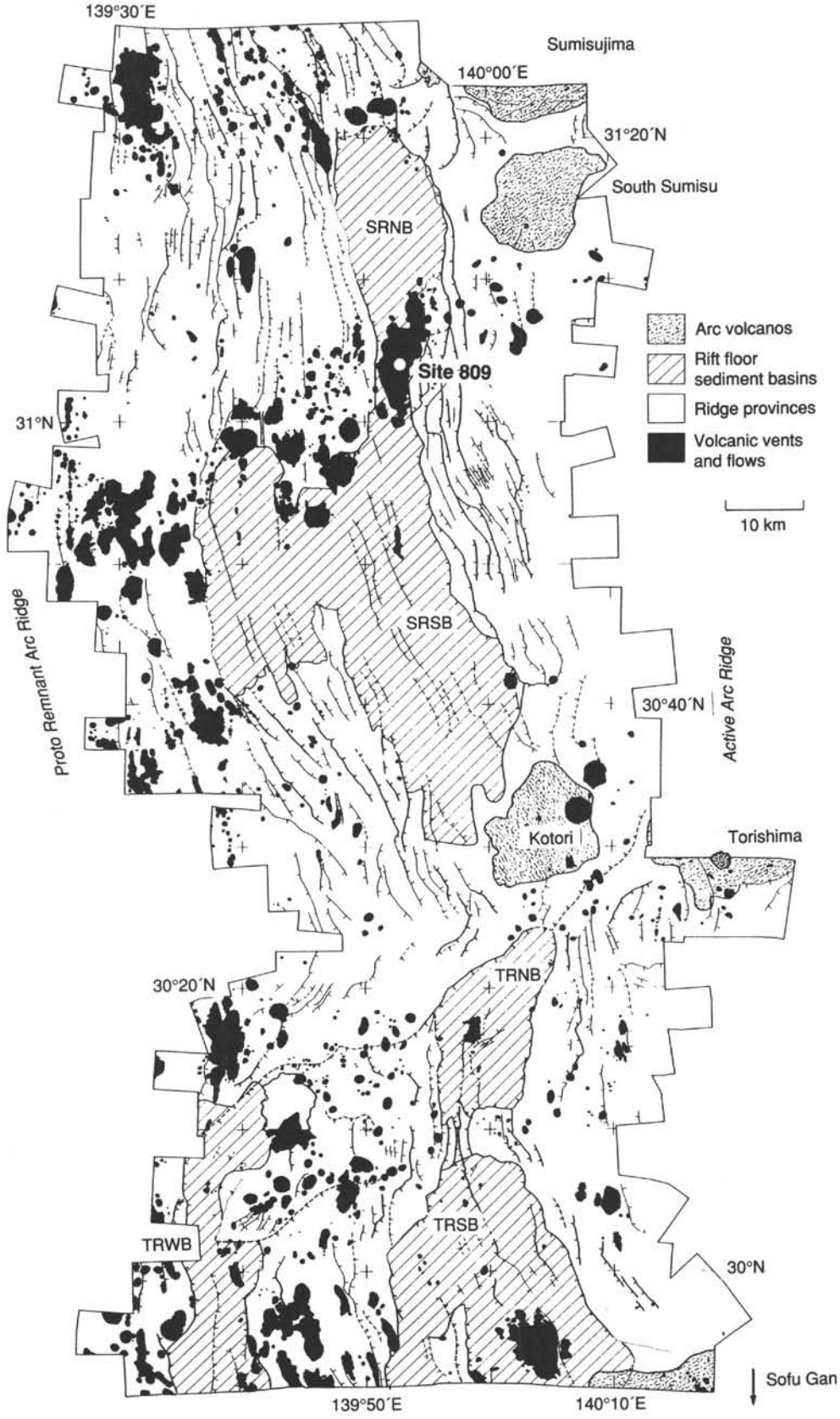

Figure 2. Sumisu and Torishima Rifts (after Taylor et al., in press) based on a colored geological map at 1:200,000 (Brown et al., 1988) interpreted from SeaMarc 1 imagery and bathymetry, plus closely-spaced single channel seismics and 3.5-kHz data. Volcanoes in the two rifts are in black. The location of Site 809 on a volcanic ridge (Central Ridge) in the center of Sumisu Rift is indicated.

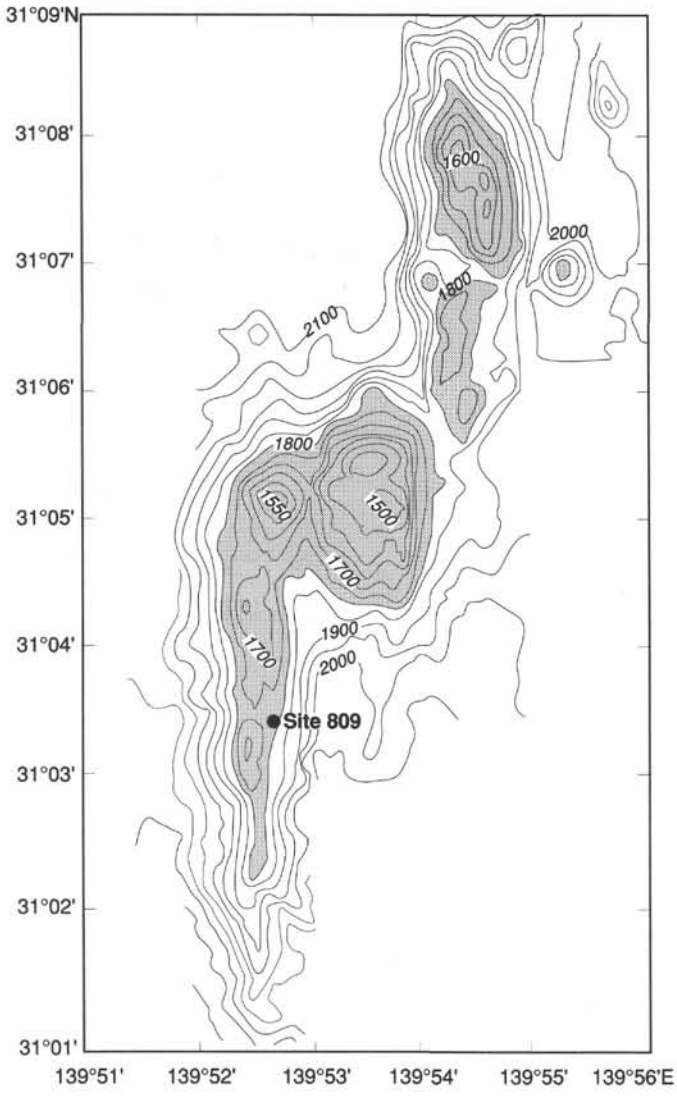

Figure 3. Seabeam bathymetry (50 m contours) of Central Ridge, Sumisu Rift (Smith et al., in press) showing the location of Site 809.

pillow lavas rather than unusual occurrences of silicic lavas (Hochstaedter et al., in press) and hydrothermal precipitates (Urabe and Kusakabe, in press) on the northernmost of the eastern row of volcanic peaks that make up Central Ridge. The site was initially targeted at a saddle between the two southernmost peaks along the western row of volcanoes, at the intersection of a *Kana Keoki* single-channel profiler record (Fig. 4) and a *Fred Moore* multi-channel seismic reflection line (Fig. 5). This was adjusted during the site approach to a location 2 km to the north, at the broader and flatter saddle between the second and third of the four coalesced volcanoes along the western fissure system (Figs. 5 and 6).

Apart from establishing the credentials of the DCS and seafloor hardware at this site, scientific objectives included determining the lithologic characteristics of very recently erupted volcanic rocks, the characteristics of incipient alteration in those rocks, and as much as possible of their chemical variation in a comparatively short vertical section. A hole 150 m deep was projected for the time planned for coring at the site. Following the coring, a logging run with a combined caliper-gamma tool was planned, chiefly to gauge hole diameter and gain experience in the use of low-weight, slim-hole logging tools in small-diameter DCS holes.

OPERATIONS

Approach to Site 809

JOIDES Resolution approached Site 809 from the north on the morning of 13 June 1990, using GPS navigation to stay as closely as possible along Fred Moore multi-channel line FM3507-8 (11-8) shown in Figure 4. We obtained a profile of the four volcanic peaks along the western fissure of Central Ridge (Fig. 7), establishing precisely the latitude of the target site at the saddle between the third and fourth peaks encountered. Turning east, we slowed, retrieved the magnetometer, streamer, and water guns, then proceeded north to that same latitude.

Turning west, we used the 3.5 kHz echo sounder and GPS navigation to establish the precise longitude of the saddle at its maximum elevation along this line of latitude. Geometrically, this represented the most level place we could find to place the HRB. Once past the ridge crest, we turned the ship 180° to 090° using a modified Oonk turn, returning precisely to a reciprocal track. Proceeding at 4 kt back to the saddle, we dropped the beacon at 1045 hr local time at the precise maximum elevation established earlier with the 3.5-kHz echo sounder. We hove to, lowered the

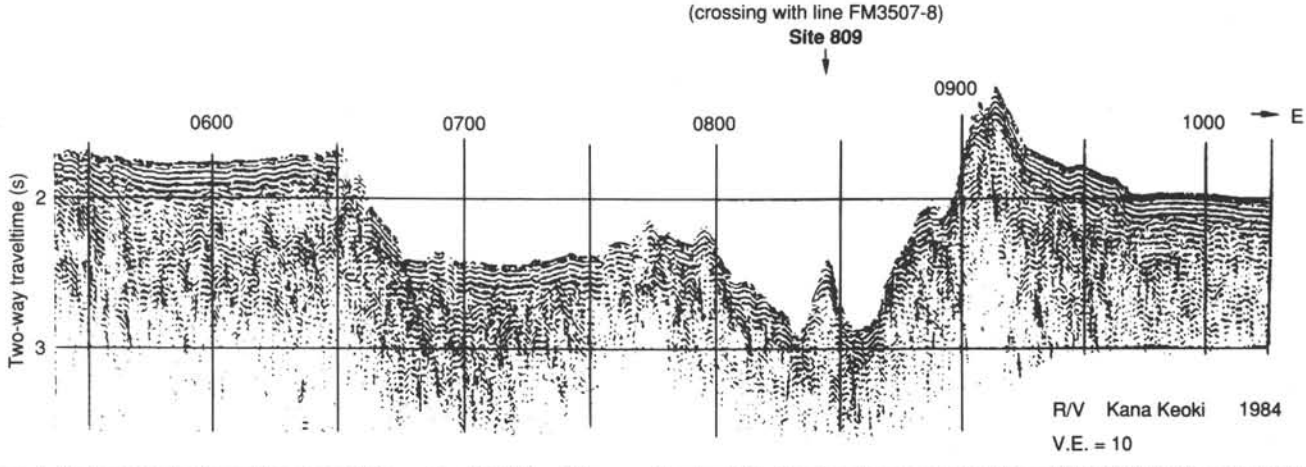

Figure 4. East-west seismic profiler record (*Kana Keoki* 84 Line G) across Sumisu Rift, showing the general location of Site 809 on Central Ridge.

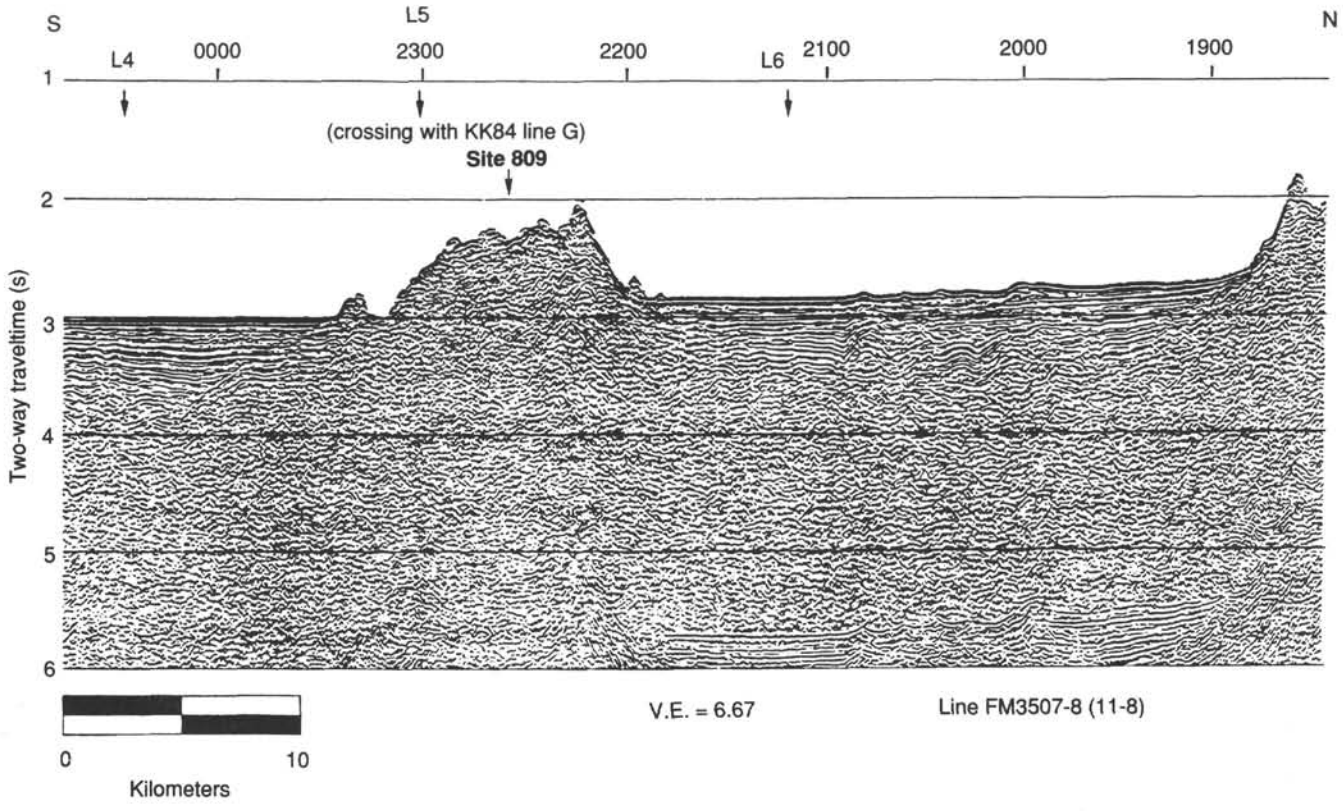

Figure 5. North-south multichannel Line FM3507-8 (11-8) across the North and South Sumisu Basins and crossing Central Ridge. The crossing with KK-84 Line G (Fig. 4) and the location of Site 809, both in saddles between small volcanic peaks, are indicated.

thrusters, and maneuvered back over the beacon. From where it was dropped, the beacon was carried by currents about 100 m to the southeast before reaching the seafloor.

Objectives of Test Holes

Prior to setting the hard rock base (HRB) at Site 809 a pair of test holes were drilled using a positive displacement coring motor (PDCM). These holes were required to aid in determining the length of the DI-BHA that could be safely drilled-in without exceeding the life of the bit and also to determine potential hole stability to avoid getting the DI-BHA stuck before reaching the proper back-off landing point. A third purpose was to evaluate the relative ruggedness of two different sizes of four-cone, tungsten carbide insert (TCI), core bits and a mating two-cone, TCI, center bit. The bits, one having an 11-5/8 in. diameter, and the other having a 9-7/8 in. diameter, used two different size bearings that required evaluation.

The PDCM used during operations at Site 809 was modified to allow dropping a series of locking balls. Dropping the balls results in locking the rotor/stator assembly and allows 25,000 ft-lb of torque to be transmitted through the motor, if required. Standard output torque for the PDCM was 6,000 ft-lb. Although available, this feature was never required during the drilling conducted at Site 809.

Hole 809A

After conducting a short TV survey, Hole 809A was established in 1819.7 m of water (adjusted to the rig floor dual elevator stool or DES). The hole was spudded on a pillow basalt surface at 0345 hr on 14 June 1990 using a PDCM and an 11-5/8 in. TCI bit with an 11-1/2 in. stabilized bit sub. The hole was drilled to 1828.0 m or 8.3 mbsf using 2,000–5,000 lb weight on bit (WOB) and a rotational speed of 30–70 rpm. The drilling took 8.75 hr

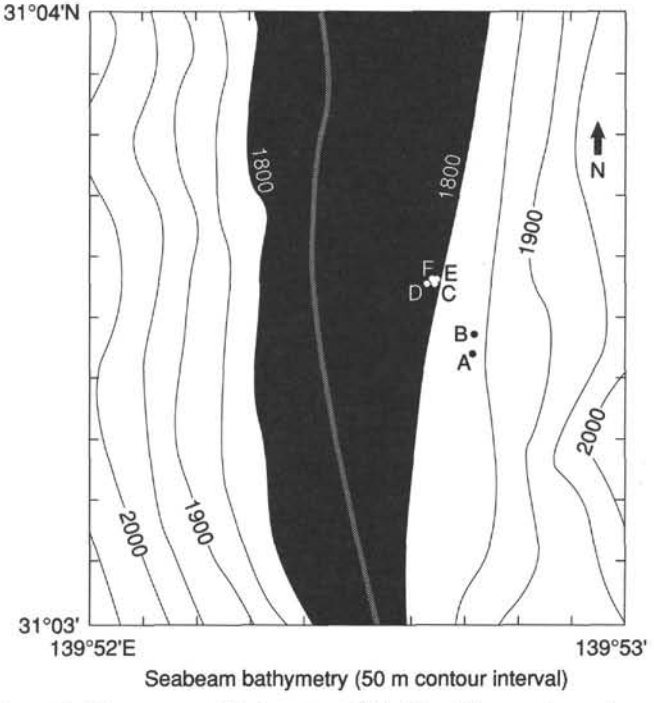

Figure 6. Enlargement of bathymetry of the Site 809 area. Area above 1800 m is black. The stippled line indicates a photogeological traverse (Smith et al., in press). The locations of Holes 809A to 809F are shown.

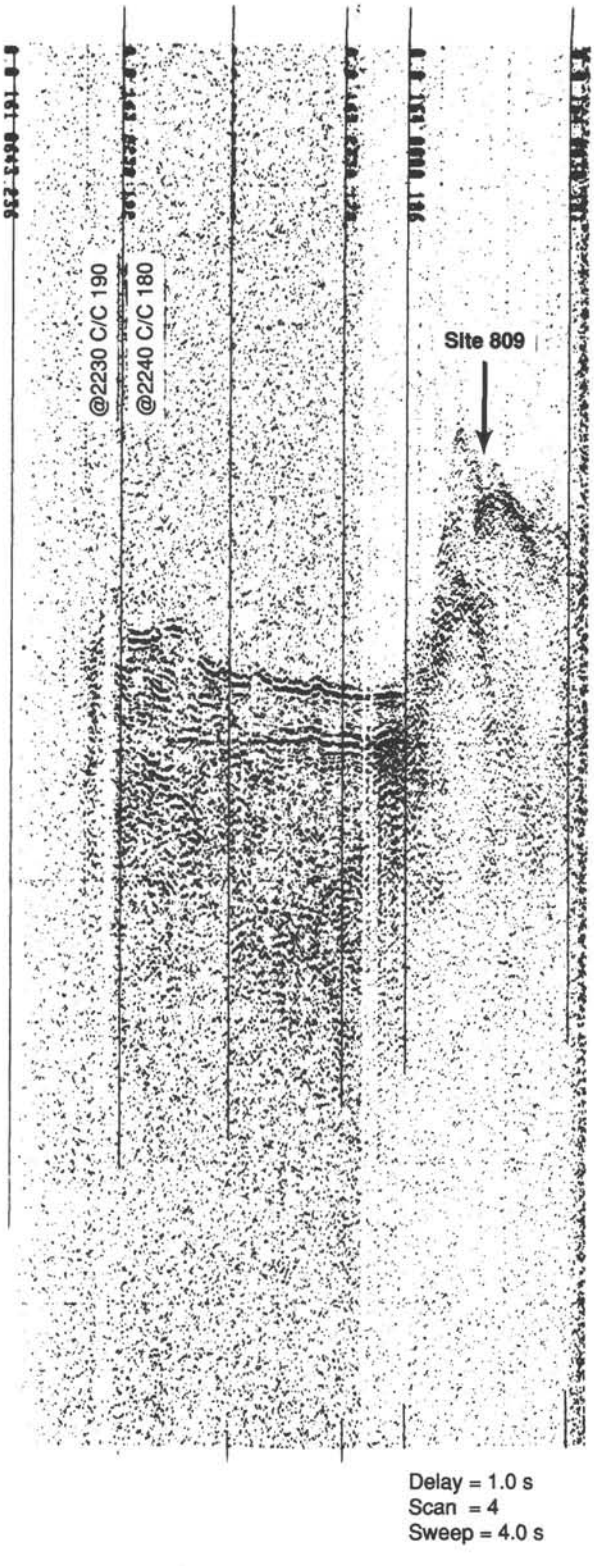

Figure 7. *JOIDES Resolution* profile of four volcanic peaks along the western fissure of Central Ridge on Sumisu Rift, showing the location of Site 809.

including several periodic stops to check on the progress with the TV camera. Although a fairly large (2–3 m) hole was wallowed out at the surface, penetration was achieved. The hole was terminated at 1700 hr on 14 June when the bit reached the rig floor. Upon recovery both primary and center bits were found to be in excellent condition and the center bit latch was functional. A small chip of vesicular basalt was recovered in the bit assembly (Table 1).

Hole 809B

After another brief TV survey, Hole 809B was established in 1799.6 m of water (adjusted to the DES). The hole was again spudded on pillow basalts at 2315 hr on 14 June 1990 using the same PDCM only this time with a 9-7/8 in. TCI bit/center bit combination and 9-1/2 in. stabilized bit sub. The hole was drilled to 1813.0 m or 13.4 mbsf using 2,000–5,000 lb WOB and at a rotational speed of 30–70 rpm. The drilling took 8.75 rotating hr. Some minor motor torquing and overpull (20,000 lb) was experienced from 3.5 mbsf down but seemed to be alleviated with the pumping of 10 bbl gel mud pills. Drilling was terminated when the bit became stuck in the hole and required 55,000 lb overpull to free. When observed with the TV camera this hole was noticeably smaller in diameter at the surface (<1.0 m). The hole was terminated at 1400 hr on 15 June when the bit reached the rig floor. Both the primary and center bits were again in surprisingly good condition and the center bit latch remained functional.

Initial HRB Installation at Hole 809C

After 2-1/2 days of assembly, welding, and ballast loading, the newly designed "mini" HRB was ready for deployment. At 1100 hr on 17 June 1990 the guide base was landed on the seafloor. Upon un-jaying from the structure, however, the cone assembly fell over, resting in one corner of the base. The floatation panels, relied upon to keep the cone vertical, had inadequate buoyancy. Several days were spent unsuccessfully attempting to right the cone structure on its gimbals and drill-in the BHA. We theorized that if the BHA were successfully emplaced it would then hold the cone structure upright and allow DCS coring operations to continue as originally planned. During the course of making one of the several near-horizontal reentries, the cone funnel structure incompletely parted from the casing hanger assembly leaving a gaping hole in the side. It was too risky to attempt reentering the structure as it was, so the bit/BHA weight was used to complete the failure, separating the funnel from the casing hanger altogether. The funnel fell to the side and came to rest upside down near the HRB.

After demonstrating that reentry into the remaining 24 in. diameter casing hanger was feasible, operations continued. Again several days were spent attempting to right the gimballed casing hanger and drill-in the BHA. Although the reentry operation itself was accomplished five times, the DI-BHA was never successfully emplaced into the seafloor. One assembly was partially drilled-in, but due to binding of the back-off nut going through the cone transition pipe, the assembly released prematurely, preventing the tensioning jay-tool and tapered stress joint assembly from engaging the hanger. This BHA was eventually fished back out of the hole. At 1130 hr on 22 June 1990 we decided to abandon efforts at Hole 809C and instead deploy the second (back-up) guide base at this site.

While tripping out with the drill string it was agreed that to make the second HRB work properly, the floatation panels from the first HRB would be required. The recovery of the parted reentry cone resting on the seafloor was considered feasible and fabrication of a fishing tool with an articulated arm commenced immediately.

Table 1. Coring summary for Site 809.

Core no.	Date (1990)	Time	Depth (mbsf)	Cored (%)	Recovered (m)	Recovery (m)
132-809A-						
1Z	14 June	1700	0.0–0.0	0.0	0.01	100.0
				0.0	0.01	100.0
132-809F-						
	Drill-in-BHA		0.0–5.9			
1Z	6 July	1230	5.9–6.2	0.3	0.13	43.0
2Z	6 July	2015	6.2–6.9	0.7	0.85	120.0
3Z	6 July	2240	6.9–9.0	2.1	0.00	0.0
4Z	7 July	0030	9.0–10.6	1.6	0.00	0.0
5Z	7 July	0620	10.6–13.4	2.8	0.00	0.0
	Center bit		13.4–13.7		(0.3 m drilled)	
6Z	8 July	2025	13.7–13.8	0.1	0.20	200.0
7Z	9 July	0225	13.8–13.9	0.1	0.20	200.0
8Z	9 July	1445	13.9–14.0	0.1	0.12	120.0
9Z	9 July	1810	14.0–14.3	0.3	0.13	43.0
	Center bit		14.3–14.4		(0.1 m drilled)	
10Z	12 July	0015	14.4–14.6	0.2	0.14	70.0
11Z	12 July	0645	14.6–17.4	2.8	1.87	66.8
12Z	12 July	0730	17.4–19.4	2.0	0.75	37.5
13Z	12 July	1200	19.4–20.5	1.1	1.35	123.0
14Z	12 July	1420	20.5–23.5	3.0	1.79	59.6
15Z	12 July	1830	23.5–23.8	0.3	0.14	46.0
16Z	12 July	2130	23.8–26.3	2.5	1.19	47.6
17Z	13 July	0000	26.3–29.3	3.0	1.48	49.3
18Z	13 July	0200	29.3–32.3	3.0	0.27	9.0
19Z	13 July	0400	32.3–35.3	3.0	0.00	0.0
20Z	13 July	0900	35.3–38.3	3.0	0.00	0.0
21Z	13 July	1515	38.3–41.3	3.0	0.00	0.0
	Center bit		41.3–41.6		(0.3 m drilled)	
22Z	13 July	2310	41.6–44.2	2.6	0.09	3.5
23Z	14 July	0200	44.2–44.7	0.5	0.00	0.0
24Z	14 July	0445	44.7–47.2	2.5	0.00	0.0
	Center bit		47.2–48.5		(1.3 m drilled)	
25Z	14 July	1145	48.5–50.5	2.0	0.00	0.0
26Z	14 July	1520	50.5–53.5	3.0	0.00	0.0
27Z	14 July	2230	53.5–59.3	5.8	0.00	0.0
28Z	15 July	0300	59.3–61.9	2.6	0.00	0.0
			61.9–74.1		(12.2 m drilled)	
29Z	15 July	1530	74.1–77.6	3.5	0.00	0.0
30Z	15 July	2030	77.6–78.1	0.5	0.00	0.0
31Z	16 July	0030	78.1–78.6	0.5	0.00	0.0
			78.6–78.7		(0.1 m drilled)	
32Z	16 July	0830	78.7–78.8	0.1	0.08	80.0
33Z	16 July	1115	78.8–79.2	0.4	0.01	2.5
[a]34B	17 July	1800	(78.6)–(79.2)			0.34
Coring total				59.0	11.13	18.7
	1881.7 (TD)		5.9	Drill-in-BHA		
	1802.5 (WD)		59.0	Cored with DCS		
			14.3	Drilled with DCS		
	79.2 m		79.2 mbsf			

[a] Bit samples from previously cored interval (78.6–79.2 m).

At 1545 hr on 23 June 1990, the failed reentry cone funnel was successfully recovered from the seafloor, after a perfect jet-sub assisted reentry into the upside-down structure. The recovery was accomplished so easily that talk turned to the feasibility of recovering the entire HRB structure itself. Since assembly of the back-up guide base would have been time consuming, and would have precluded an HRB deployment at the M.I.T. Guyot bare rock site, it was decided to attempt the first-ever HRB recovery.

After reentering the inclined casing hanger for the fifth time, the jay-tool was engaged, and the guide base from Hole 809C was lifted from the seafloor. At 0745 hr on 24 June 1990 the guide base was landed safely on the moon pool doors officially terminating Hole 809C.

Repaired HRB Installation and Jay-tool Failure at Hole 809D

It took just over 28 hr to repair the recovered HRB and mount the second set of floatation panels on the refurbished cone funnel. In addition, a shipboard-designed and fabricated tilt beacon was installed on the HRB structure. After one abortive attempt to land the HRB (due to excessive slope), the guide base was released at the seafloor on 25 June 1990 at 1630 hr. The additional floatation worked as planned, and the cone remained vertical as the drill string was removed from the hanger assembly. A few minutes were taken to view the tilt indicators on the side of the guide base with the TV camera. The indicators, fabricated from chain, indi-

cated that the structure was resting well within the limits of the gimbal assembly.

At 0600 hr on 26 June 1990 the HRB was reentered with the DI-BHA and Hole 809D was spudded in 1802.0 m of water. It took only 3/4 hr to drill-in the 11-5/8 in. asswembly to 1808.3 m or 6.3 mbsf. The DI-BHA system worked perfectly this time giving a characteristic pump pressure increase as the PDCM torqued up to unscrew the back-off nut, then dropping as the BHA was freed from the rest of the drill string.

At 1615 hr on 26 June 1990, the cone was reentered with the jay-type tensioning tool and tapered stress joint. Apparently during the reentry/jay-in process, the dogs on the jay-tool were damaged. Upon un-jaying, a large white object was observed dropping into the hole. When the tool was recovered on-deck, it had one missing jay-dog and one missing dog cage arm. After several repeated attempts to recover the center bit, it was determined that the junk must have lodged in the throat of the lower back-off nut preventing access to the center bit. The decision was made to terminate Hole 809D and move the guide base once again. At 1830 hr on 26 June 1990, the guide base was stripped over the drilled-in BHA and moved 10 m south of the original landing spot completing operations at Hole 809D. After moving the guide base, the DI-BHA could be seen with the jay-dog resting squarely on top of the lower back-off nut, just as suspected. The BHA appeared to have been drilled-in perfectly straight with negligible evidence of washout or wallowing.

Formation Collapse Beneath the HRB at Hole 809E

Buoyed by the success of drilling in the BHA on the previous hole, the pipe was round-tripped and another 11-5/8 DI-BHA was deployed. This time the BHA was spaced out to be 9.0 mbsf, hoping to reach more consolidated formation than was found on earlier holes.

The guide base was reentered at 0645 hr on 28 June 1990 and Hole 809E was spudded. The first several meters of drilling proceeded smoothly, however it soon became evident that conditions were not the same as on previous drilling efforts. After 14 hr of drilling and several restarts, suspected at the time as the result of hole caving problems, the hole was still a good meter short of reaching the required back-off depth. This hole was characterized by high, erratic torque, pipe sticking, and the usual problems associated with attempting to drill unstable fractured crystalline formations. At 2130 hr it was decided that the DI-BHA should be recovered and inspected rather than risk leaving a bit cone in the hole or backing-off prematurely.

When it was recovered on-deck, it became evident that the assembly had been in a bind during drilling with scars and metal shards prevalent on the back-off assembly. It was obvious that something was wrong downhole so the drill string with jay-tool and TV system were deployed to inspect the condition of the HRB. Upon inspection of the seafloor it was discovered that the guide base had shifted dramatically from its original attitude during the drilling process. Evidently the vibration, circulation, or a combination of the two had caused two of the four HRB legs to punch through the pillow basalts and the resultant angle exceeded that which the gimballed cone could accommodate. This resulted in putting a metal-to-metal bind on the DI-BHA during the drilling process which was excessive enough to prevent proper seating of the back-off assembly. All further progress of the borehole was stopped when the guide base shifted. Based on these observations, the guide base was again moved and at 1230 hr on 29 June 1990, Hole 809E was ended.

DCS Coring at Hole 809F

With the HRB lifted off bottom, the ship was offset 20 m to the west. During the move the signal from the tilt beacon returned, probably as a result of cuttings being washed from above. The HRB was landed once again on the seafloor at 1300 hr. Upon touchdown, the camera frame swung as if the pipe was bowing, a corner of the base became visible from beneath the cone funnel, and the tilt beacon changed repetition rate. All of these signs indicated that the guide base was sitting at an excessive angle. The base was picked up for the second time, and the pipe was allowed to swing free for a few minutes. When the base was landed again, approximately 5 min later, all indications were that the base was at an acceptable attitude. When the pipe was un-jayed, the dogs could be seen freely sliding in the jay-slots and the cone appeared vertical.

After the un-jaying operation was completed, 45 min was taken to maneuver around the guide base and attempt to determine its attitude. The northwest side appeared to be dipping 4°–5° to the west, the northeast side appeared to be dipping 12° to the east. While we were viewing the northeast side, the north leg appeared to punch through a basalt pillow. The resultant dip changed from 12° to 9°–10°, still to the east.

After a round trip of the drill string, the pipe was run back to bottom with the DI-BHA). A TV reentry was made at 2215 hr on 29 June 1990, Hole 809F was spudded 5 min later, and the DI-BHA was drilled-in and released by 2250 hr. Thirty minutes was required to drill-in the assembly 5.9 m using the PDCM.

After pulling out of the cone, 15 min was taken to check the attitude of the cone. The dip angles were found to be the same as before drilling, and the drill string was then tripped back to the rig floor.

The tensioning sub/tapered stress-joint assembly was made-up and the drill string was run in the hole. The cone was reentered at 0815 hr on 30 June, the tension sub was then jay-ed in, and 35,000–40,000 lb tension was applied. Since this was the first attempt to impose tension on the drill pipe, measurements were made to determine the final space-out of the DCS platform when hung in the derrick. This was done while running in the hole with the sinker-bar assembly to recover the center bit and latch assembly from the DI-BHA. Upon recovery of the center bit, the string was un-jayed from the guide base and the top drive was set back. Prior to pulling out of the hole with the drill pipe, the VIT frame was recovered and the drill line was cut and slipped. By 1230 hr the pipe was on-deck and preparations for DCS drilling were begun.

Prior to picking up the DCS platform, several operations had to be performed. These included removing the iron roughneck "big-foot" and dual-elevator handler from the drill floor, installing the platform dolly tracks on the rig floor, skidding the DCS platform over well center, and installing the guide dolly arms on the derrick guide rails.

Because this was the first time the platform was picked up, several other "first time" tests were run. The platform was picked up as far as possible until the travelling block was at the crown. No interferences were discovered although we found that tie backs would have to be adjusted on the primary heave compensator hoses. Some secondary (safety) stops were fitted and welded onto the platform. The shock-cylinder relief valves were set, and the DCS standpipe hoses were installed. In addition, a DCS wireline winch test was conducted while the platform was over well center.

After completing all required preliminary DCS testing and installations, the platform was racked back to the starboard side and preparations were made for tripping the DCS tubing string. With the drill pipe positioned above the seafloor, the 90 ft stands of 3-1/2 in. tubing were tripped into the hole. By 1530 hr the tubing was tripped down to the top of the stress joint and hung off at 1791 m. The tubing running tools and staging were then rigged down.

The DCS platform was rolled into place over well center and the guide-dolly roller assemblies were installed onto the derrick guide rails. The 500 ton links were attached between the heave compensator and the DCS mast. The platform was picked up in the derrick and the lower set of 500 ton links were pinned into the lower end of the mast. The DCS platform was raised high enough in the derrick to allow the Varco top drive to be picked-up and attached to the links below the DCS platform.

With the DCS platform positioned approximately 45 ft above the rig floor, the laborious, time-consuming strip-over operation was begun. By 1700 hr on 2 July 1990, the stage was set for the 21st reentry of the site.

At 1715 hr the cone was reentered, the jay-tool attached, and 35,000 lb of tension was placed on the tapered stress joint. Prior to beginning continuous DCS platform operations, a safety meeting was held with all ODP and SEDCO/FOREX crew members involved to discuss emergency procedures to be followed in case a drive-off or platform fire should occur.

With all safety procedures in place, the DCS rig crew began conducting off-bottom tests of the secondary heave compensator. A leak in the DCS standpipe manifold was repaired, and pump tests were conducted with and without the DCS core barrel in place. These were done to establish baseline pressures at various flow rates to aid in deciphering potential core blocks or other downhole problems once coring was initiated. After adjusting the lebus-winch counter-balance weights on the DCS wireline winch and conducting a series of other compensator tests, the first attempts at coring began.

At 1930 hr on 6 July 1990, the formation was tagged with the DCS bit for the first coring attempt. A Longyear Series-2 impregnated bit (3.960 in. OD × 2.2 ID) was used for bit run No. 1. The 10 ft drilling joints were tripped to the bottom of the DI-BHA rathole at 5.9 mbsf using the secondary heave compensator to slowly feed the drilling assembly through the void between the bottom of the tensioning tool and the top of the back-off sub. No difficulty was encountered lowering the bit through this section. The 10 ft joints were advanced to the casing shoe and the secondary compensator was engaged. However, the computer repeatedly would instruct the bit to touch bottom, then retract it. An increase in pump pressure occurred, indicating a core jam. The core barrel was recovered and found to have 13 cm of vesicular basalt rubble in the barrel of Core 1Z (Table 1). Repeated indications of core jams were reflected by pump pressures. The second core barrel was pulled, but was empty. We suspected that the rubber core-block washers were in some way causing false indications of core jams so they were replaced with steel washers. It was recognized that without the rubber washers it would be more difficult to see the core blocks. The next core barrel run resulted in the recovery of 0.85 m of fractured basalt. Baravis polymer drilling fluid was circulated continuously during the coring cycle. Typical coring parameters were 20 gpm circulation, weight on bit from 1000 to 2000 lb, bit rotational speed from 80 to 100 rpm, and pump pressure from 80 to 280 psi.

After limited recovery on the first two coring runs, no additional core was recovered for the next four coring runs (Table 1). It was initially thought that the core barrels were not latching in. The space-out on the inner tube was shortened up by 0.625 in. in an attempt to correct the erratic pump pressures observed. During coring runs 3 through 6, pump pressures varied from 200 to 750 psi. Numerous center-bit runs were made to clear any obstruction that might be in the bit. The core barrel latch dogs, landing shoulder, and core catcher were painted prior to dropping the barrel. This gave a positive indication when the barrel seated properly. On coring run 6, difficulty was encountered latching onto the core barrel with the overshot. Apparently there was a significant amount of fill on top of the core barrel. Two wireline runs were made in an attempt to pull the core barrel. We decided to swab the pipe using a core barrel latch-head assembly in an attempt to clear the fill above the core barrel. The swabbing attempt worked, and the core barrel was recovered. Coring operations were resumed and four more cores were recovered with recovery ranging from 0.2 to 2.0 m. Again, pump pressures were very erratic. Coring parameters were as follows: flow rates varied from 20 to 70 gpm, bit rotational speeds ranged from 80 to 200 rpm, and pump pressures ranged from 150 to 750 psi. The drilling rate fell off significantly during the last three coring runs for this bit. On the last run, Core 132-809F-9Z, the bit advanced only 0.3 m in 45 min, whereas only 15–20 min were required to advance the bit 1–2 m, earlier in the bit run. Core No. 9Z recovered 0.13 m of massive basalt. We decided to pull the bit at the end of that run since bit failure was suspected.

The first DCS bit arrived on-deck at 2400 hr on 10 July. About 70% of the usable bit matrix was worn away, limiting the flow paths across the face of the bit. This explained the high pump pressures that occurred at the end of the bit run.

All core-barrel components were checked and space out reverified. A new impregnated bit was installed and the tubing was tripped back in the hole. At 0500 hr on 11 July 1990, the tubing was down and the DCS platform was again ready to be picked-up. At 1630 hr that same day the cone was reentered, the jay-tool was engaged, and tension of 35,000 lb was pulled.

After another round of mud-pump flow tests, heave-compensator tests, and trouble-shooting of the top-drive control system, DCS coring with the second bit was ready to begin.

The second bit run was made with a Longyear Series-2 impregnated bit identical to that used in the first bit run. There was nothing unusual about the wear noted on the first bit to indicate that a change in the bit matrix or crown design should be made. Once outside the casing shoe, the computer for the secondary heave compensator was used to lower the bit to bottom while rotating at 100 rpm. A center bit was in place for this operation. While rotating through the casing shoe and down to the bottom of the hole, up to 2000 ft-lb of torque occurred. The high torque was attributed to the absence of lubrication in the annulus between the tubing and drill pipe. This may have been accentuated by ocean currents of 1.5–2.0 kt bending the drill string. After pumping EP Mudlube mixed with Baravis polymer into the annulus, the high torque dissipated. When bottom was tagged, 3.0 m of fill was encountered. Once on bottom, the center bit was retrieved and coring operations were resumed at 0600 hr on 12 July 1990. Nine consecutive cores were cut beginning with Core 132-809F-10Z. Drilling parameters were as follows: weight on bit 500–2000 lb, flow rate 30–50 gpm, bit speed 100–300 rpm, and pump pressures from 100 to 300 psi. Core recovery ranged from 0.14 to 1.87 m of highly fractured and vesicular basalt in each 3 m core.

After advancing the hole 32 m beyond the casing shoe, core recovery suddenly dropped to zero. Apparently a zone of highly friable volcanic tuff and unconsolidated basalt breccia was encountered.

Beginning at 1630 hr on 13 July, intermittent DCS coring was resumed alternating with testing of the new secondary heave compensator. During this period, numerous attempts were made (including dropping the bit deplugger and center bit) to clear any possible obstruction that might have prevented the core barrels

from latching in. The thinking was that this might be the cause of the nil core recovery. Many variations of bit speed, flow rate, and weight on bit were also used, all to no avail. Some intervals were drilled ahead with a center bit, others drilled ahead with core barrels in place. At one point a push sampler was deployed; then a modified bit deplugger with a hole bored in the bottom was used. Several make-shift core catchers were tried, all with little or no success. The only common thread throughout this period was an extremely high penetration rate and indications of voids ranging in size from a few tens of centimeters up to nearly a meter. Penetration rates were so excessive that selected weight on bit could not be maintained even with full DCS hydraulic power advancing the bit.

A drift profile of the hole at 60 mbsf was attempted but the results were inconclusive because of a bubble in the angle unit. The best interpretation is that the hole deviated from the vertical by about 1.5°.

Finally, out of desperation, the flow rates were continually decreased on the last few cores in an attempt to recover the elusive material. Cores 132-809F-29Z through -33Z were cut with minimal (10.0 gpm) to below minimum (6.0 gpm) flow rates as recommended by the bit manufacturer. All that was accomplished was that the penetration rate went to zero and the bit stopped drilling nearly entirely. The second-to-last core recovered a chunk of vesicular basalt jammed in the core catcher with impressions of the center-bit surface-set diamonds imbedded in it. The center bit had been run just prior to that core. The last core recovered a few pebbles of vesicular basalt. Apparently, the DCS bit had finally penetrated the friable volcanic breccia back into more massive vesicular basalt just as the flow rates were cut back. Due to indications that the bit was plugged after Core 132-809F-33Z, and a suspicion that bit failure had also occurred, based on penetration rates, the bit run was ended. All coring operations were suspended at 2015 hr on 16 July.

Upon completion of coring operations, several attempts were made to run the caliper/gamma slimhole logging tool through the DCS bit. These attempts were unsuccessful, making it necessary to trip the DCS tubing out of the hole. This tubing trip was "wet" for all but 37 stands (water would spill from each disconnected piece of tubing) because of an obstruction at the bit. At this point the obstruction cleared itself, and the remainder of the trip was "dry."

Examination of the bit, which arrived on-deck at 0400 hr on 18 July, revealed that all of the diamond-impregnated matrix was gone. A piece of basalt 0.34 m long was found trapped inside the bit throat. We do not know at what point the bit actually failed. It is possible that it failed prior to passing through the unconsolidated zone as evidenced by the extremely long drilling times that were required to advance the bit for the last two cores. A total of 13.4 hr rotating time were logged during the bit run. It is also possible that coring the breccia zone may have prematurely eroded the matrix of the bit to the point that, when competent basalt formation was finally encountered near the bottom of the hole, the bit had little or no drilling life remaining. The mode of failure also may have been abrupt separation or loss of the bit crown due to drilling without adequate flow rate to clean and cool the bit matrix.

In all, 33 DCS cores were taken on Hole 809F (Table 1). A total penetration of 79.2 m was achieved with 59.0 m cored, 11.13 m recovered, and 14.3 m drilled. All but 32 m of the hole was drilled through the elusive, unrecoverable, volcanic breccia.

We continued with logging. Because of the repeated attempts to break through the obstruction at the bit with the logging tool, 75 m of kinked logging cable had to be removed and the seven-conductor logging line reheaded. Beginning at 0400 hr on 18 July 1990, several attempts were made to run the logging tool down the drill pipe string into open hole. However, a bridge was encountered at the top of the hole. Lowering the logging tool onto the bridge only succeeded in lowering it by a few meters, but no farther. With this, logging was abandoned at Hole 809F.

The third and final rendezvous of the leg occurred on 15 July 1990, when the *No. 21 Chitose Maru* returned to Site 809 for the second time. The vessel brought fresh fruit and vegetables to the SEDCO/BP 471 and received two disembarking passengers, Messrs. McKinnon and Dominguez. Dr. McKinnon was returning to WESTECH having completed his work on the DCS secondary compensation system. Mr. Dominguez, a SEDCO oiler, was encouraged to leave by the ship's doctor due to the possible recurrence of a serious medical condition. There was no medical emergency at the time.

After pulling out of the hole with the tensioning sub and tapered stress joint, the drill collars racked in the derrick were laid out and the upper guide horn was installed. The DCS platform was set back, and the vessel got underway for Site ENG-6, Shatsky Rise, at 1845 hr on 18 July 1990.

Comparisons with Previous Drilling Attempts in Young, Fractured Basalt

Throughout both DCS bit runs, hole stability was not a problem. Very little fill was encountered, and the DCS tubing string was never subject to excessive torquing or pipe sticking. As mentioned above, when drilling with the 11-5/8 in. drilling assembly in Holes 809A and 809B, both hole sloughing and stuck pipe occurred within 9 m penetration below the seafloor. During Legs 106 and 109, we found that, when drilling fractured basalt formations, a smaller hole size enhances hole stability. If reducing the hole size from 14-3/4 in. to 9-7/8 in. enhances hole stability, a further reduction from 9-7/8 in. diameter to 4 in. might create hole conditions that would allow significant penetration into fractured basalt. This premise was borne out by the results of drilling with the diamond coring system at Site 809.

LITHOSTRATIGRAPHY AND IGNEOUS PETROLOGY

Beneath the casing shoe at 5.9 mbsf, a total of 73.3 m of igneous material was either cored or drilled in Hole 809F. Three general intervals in the hole can be defined based on coring rate, recovery statistics and material recovered. These are (1) 5.9–29.3 mbsf — a sequence of pillows or thin flows which drilled alternately fairly rapidly and slowly, and which gave fairly high recovery using the DCS; (2) 29.3–78.8 mbsf — a sequence of extremely easily penetrated material which took only small weight on bit and gave essentially no recovery; and (3) 78.8–79.2 mbsf — a basalt flow which drilled fairly slowly, and in which the second bit failed. The long interval of virtually no recovery is probably a vitroclastic tuff or breccia formed of highly vesicular and expanded fragments of glassy basalt. A few small scrapings of sandy material obtained from the walls of two core barrels run in this interval include basaltic glass. The rocks described in the remainder of this section are from the first and third of these intervals.

Lithology

A representation of the basalts recovered by diamond coring from Hole 809D is shown in Figure 8. The two intervals with significant recovery are separated by a friable formation (Cores 132-809F-19Z to -33Z) which yielded a few small pieces of basalt (Cores 132-809F-22Z, -32Z, and -33Z) plus tiny amounts of sand- to silt-sized grains of quartz and plagioclase, glass shards, scoria, heavy minerals, and drilling debris (pipe scale, paint chips). Much

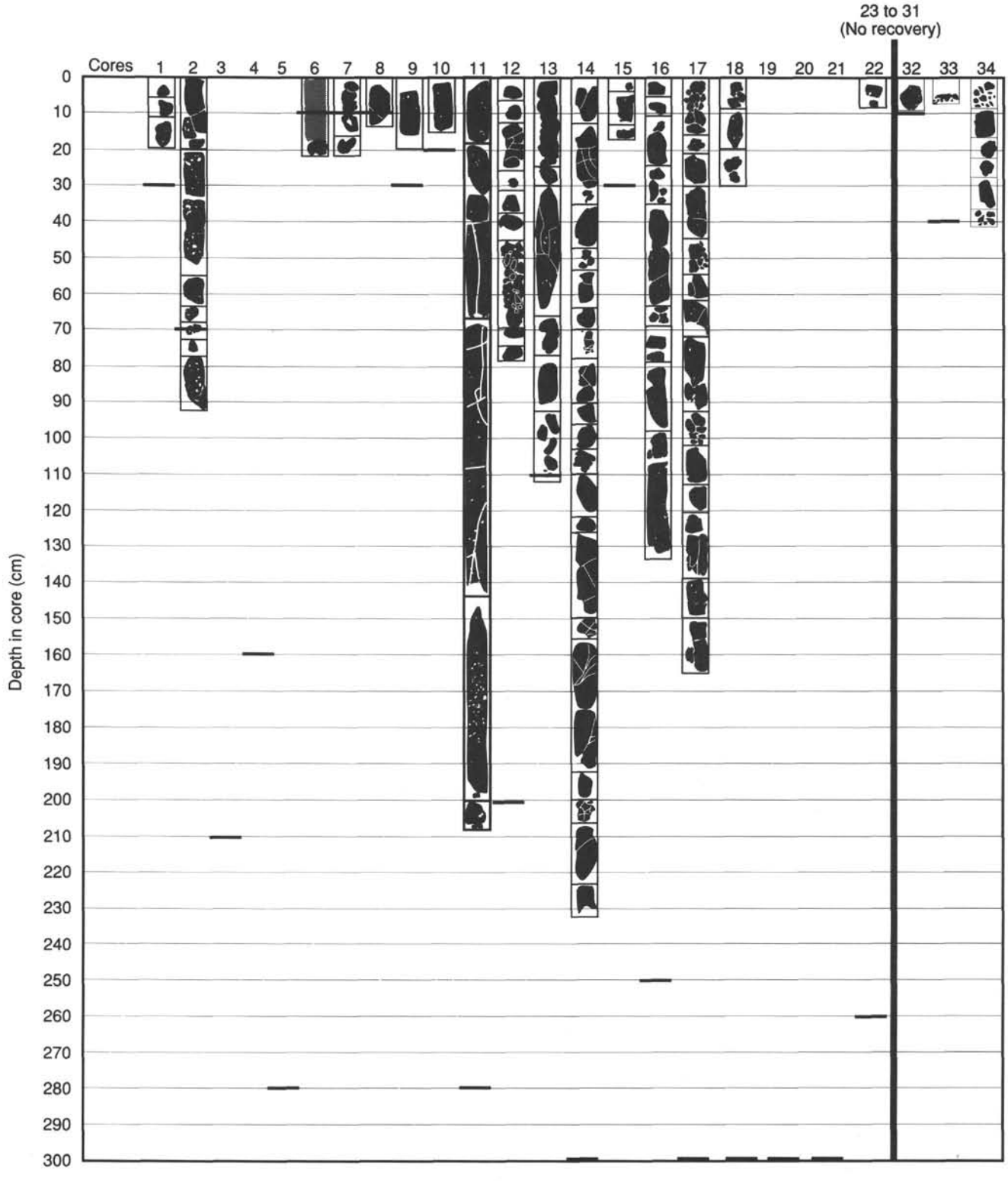

Figure 8. The aphyric basalts (black) and cuttings (stippled, Core 132-809F-6Z) recovered during diamond coring at Hole 809F. Major vesicles and fractures are indicated in white. The short black lines indicate the depth cored. Core lengths longer than depth cored are a consequence of spacing of pieces in the core liners. Illustrations are from scanned line-drawings of the core photographs used in preparing the barrel sheets.

of the sand was probably produced by the action of the drill; the source of the quartz is enigmatic (contamination from bentonite mud?).

The rocks are consistently fresh, microcrystalline basalts. Only two phenocrysts, under 2 mm in size, were found in hand specimen (but see "Petrography" section below). The first was an olivine grain in Section 132-809F-8Z-1; the second was a plagioclase grain in Section 132-809F-32Z-1.

Surfaces of individual pillows or flows (cooling units) were identified by the presence of an altered surface or a quenched margin at the top or bottom of a core piece. The basalt flows at Site 809 have nearly horizontal cooling-unit boundaries as close as 10–15 cm apart. The short core pieces from between 14 and 29 mbsf often have clay alteration on the upper and lower surfaces. Four samples have glassy margins and concentric zones of vesicles, a characteristic of pillowed basalts (Figs. 9 and 10).

The basalts at Site 809 are fractured. This is evident by altered surfaces within the cores. Core 132-809F-11Z (Fig. 8) from 15 mbsf has vertical fractures with minor clay alteration. Despite these uncemented horizontal and vertical discontinuities in the basalt, the DCS performed well in this interval and the recovery rate was over 50%.

The abundant vesicles in these island-arc rift basalts resemble those described in highly volatile basalts from more mature back-arc basins with well-defined spreading centers (e.g., Mariana Trough and the Shikoku Basin (Garcia et al., 1979; Dick, 1980). Small "pinhole" vesicles (Fig. 11) are common in all the basalt samples. The spherical or somewhat irregular openings, which are less than 1 mm in size, are uniformly distributed in most samples. Large (>1 cm) vesicles are found in only a few samples and are most common in the upper section of the hole. The cavities are often partially filled with vesiculated residual melts. Such vesicles are known as "segregation vesicles" and occur at several places in the upper cores (e.g., Figs. 11 and 12). The infiltration phenomena has been attributed to a reduction in confining pressure on the gas during intrusion of already vesiculated magma (Smith, 1968; Sato, 1979).

Segregation vesicles can be partially filled with vesiculated basalt. In many, the melt has collected on the floor of the vesicle (Figs. 11 and 12). The residual deposits are geopetal structures indicating the direction of top during the solidification of the flow. They are horizontal with respect to the cored side of the rock, thus top is up.

Residual melts have also invaded cooling fractures in the basalts. A vesiculated vein of basalt, not greater than 1–2 mm in width, was found in the flow at 13.9 mbsf (Core 132-809F-8Z). Fine vesicle trails, spaced approximately 2 cm apart, angle through many of the cores. The trails plunge about 60° from the vertical and resemble the small lines of gas bubbles that form in a glass of beer. The high slope of the trails might be caused by the laminar flow of the basalt. These features might also be fine cracks that have annealed with vesiculated basalt.

Large (>1 cm) inclusions of vesiculated basalt occur in the upper cores. These typically have a smooth rounded perimeter and show no petrologic variation from the country rock in macroscopic appearance (Figs. 11 and 12). Unlike segregation vesicles which were infiltrated with melt, these inclusions are pieces of partially crystalline basalt that were incorporated back into the solidifying melt. They are more vesicular than the surrounding basalt, thus may have been relatively buoyant.

Alteration and hydrothermal products, including pale green smectites and iron-oxyhydroxides, occur on fracture surfaces and as amygdules in isolated vesicles. An elongate vesicle from Core 132-809F-11Z has red acicular microcrystals (Fig. 13). The needles appear pasted together by a clear silica-like mineral. A large cavity from Core 132-809F-17Z has a bubbly light-grey

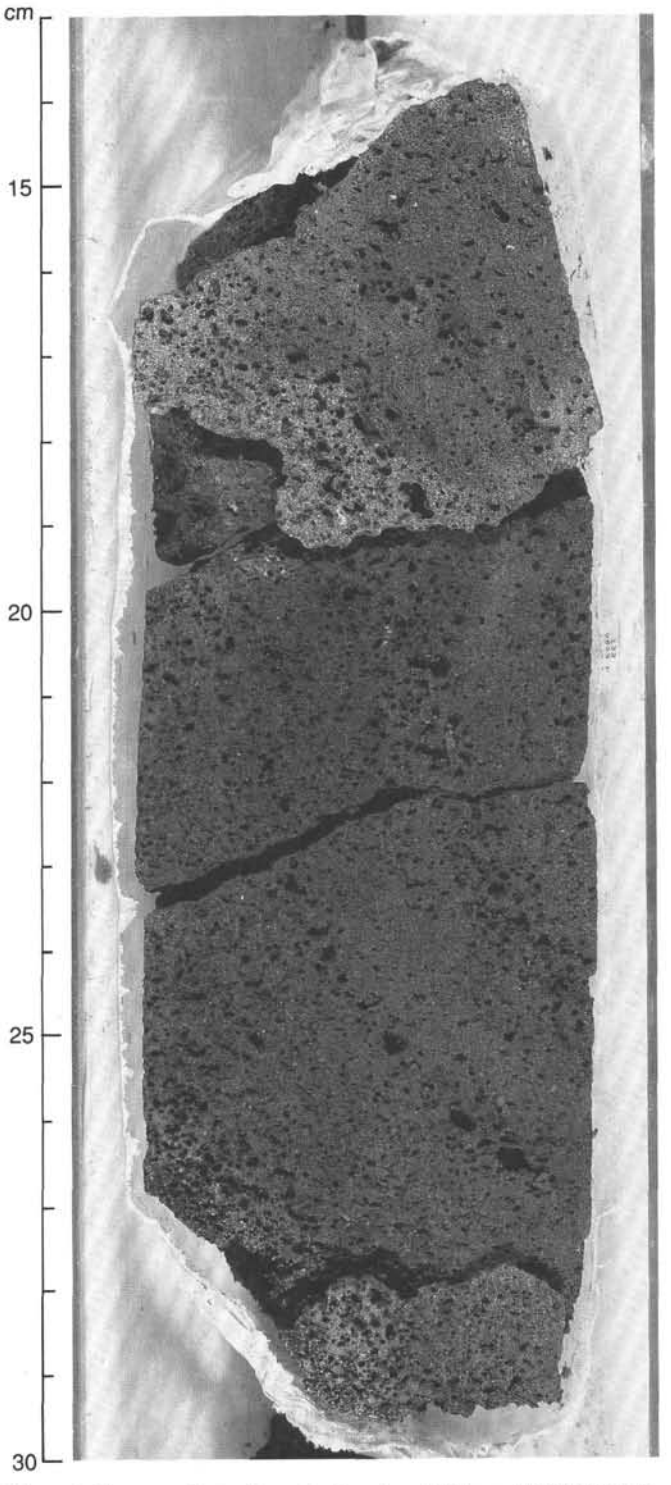

Figure 9. Close-up photo of cored pillow basalt (Interval 132-809F-14Z-1, 14–30 cm).

precipitate along the walls (Fig. 14). Two vesicles further down in Core 132-809F-17Z are lined with yellow-green clays (Fig. 15).

Petrography

Basalts from Hole 809F are aphyric, or extremely sparsely phyric, vesicular fragments of pillows, thin flows, and probably

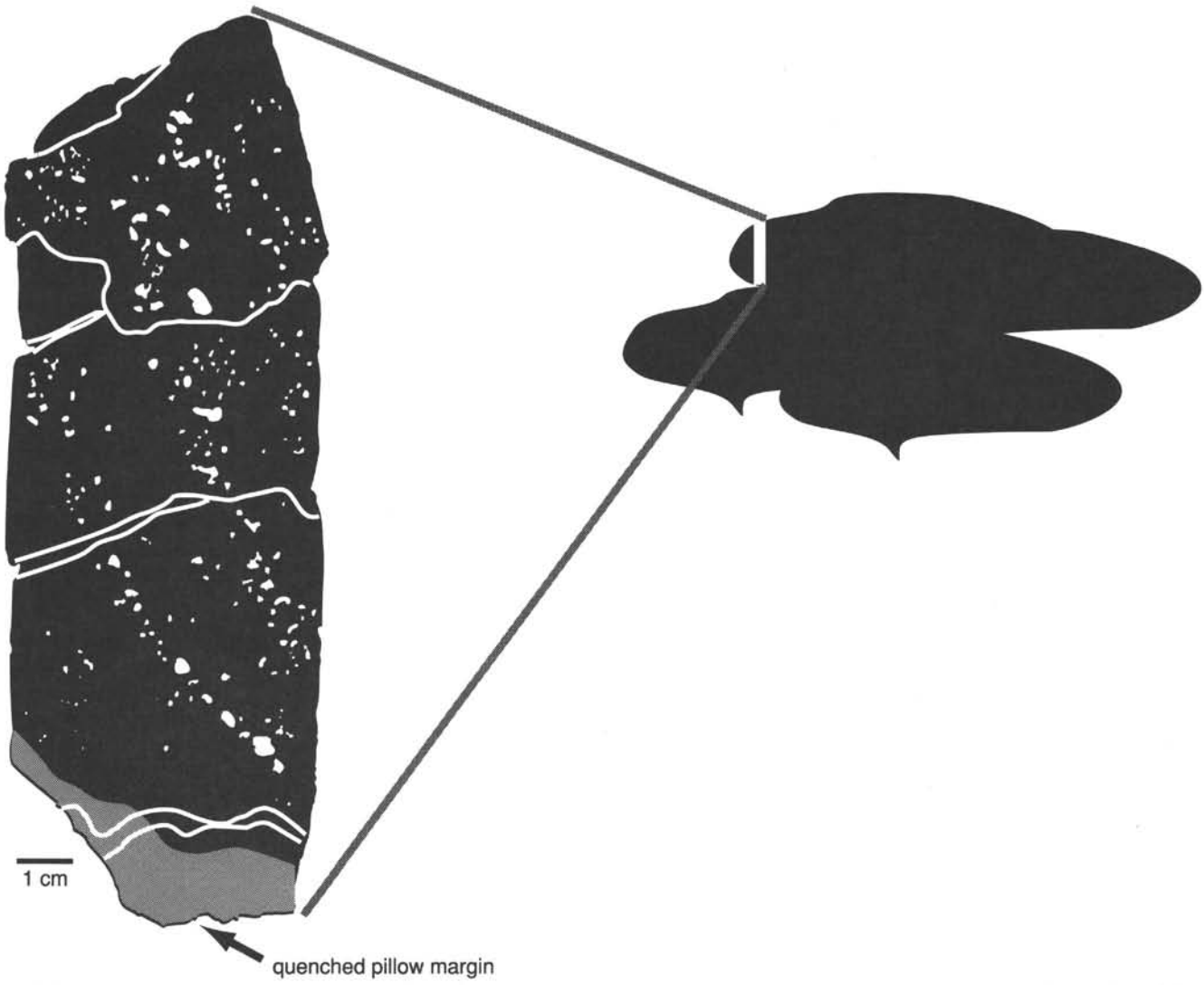

Figure 10. Line drawing of the basalt from Core 132-809F-14Z in Figure 8 showing a quenched margin. Note the concentric zonation in the vesicles indicative of a pillow structure (cartoon).

breccias. There are two general types of basalt, which we term ferrobasalt (5.9–21.0 mbsf) and olivine tholeiite (21.0–79.2 mbsf) based on a combination of petrography and chemical compositions. The olivine tholeiites actually comprise two slightly distinctive chemical types, but these are virtually identical in thin section. Petrographically, the only evidence of the geochemical distinction between ferrobasalts and olivine tholeiites is the presence of fairly rare (<5%) olivine crystals in the olivine basalts, whereas this mineral is absent in the ferrobasalts. Two other features of the ferrobasalts, however, are also related to composition. These are (1) comparative abundance of titanomagnetite; and (2) consistent development of large segregation vesicles. These features are only evident in fairly crystalline pillow/flow interiors.

There are rare and highly scattered skeletal microphenocrysts of plagioclase in both basalt types, but the rocks consist primarily of intergrown microlitic plagioclase and subhedral to dendritic clinopyroxene crystallized at high cooling rates. One olivine tholeiite contains a 0.5 cm glomerocryst with plagioclase and clinopyroxene. The rocks clearly were multiply saturated in both phases on quenching. Olivine tholeiites additionally were saturated in olivine, but they contain no spinel. In general, plagioclase is modally more abundant than clinopyroxene, in the ratio of about 3:2.

All of the coarser-grained rocks contain variable proportions of intersertal material depending again on cooling rate (distance from the margins of individual pillows or flows). This consists primarily of dendritic to spherulitic clinopyroxene, acicular to feathery plagioclase, spectacularly skeletal titanomagnetite, and variable amounts of glass. Tiny rods of ilmenite and small spherules of pyrrhotite also can be seen in the vicinity of skeletal titanomagnetites using reflected light.

In the ferrobasalts, there are two generations of titanomagnetite. The first is fairly large, and has euhedral to skeletal morphologies. If not on the liquidus with plagioclase and clinopyroxene, it was close to it. The second generation is much smaller, and highly skeletal, occurring in intersertal spaces as well as in segregation vesicles and veinlets.

Considering the two types of basalt to represent different stages along a liquid line of descent, the overall crystallization

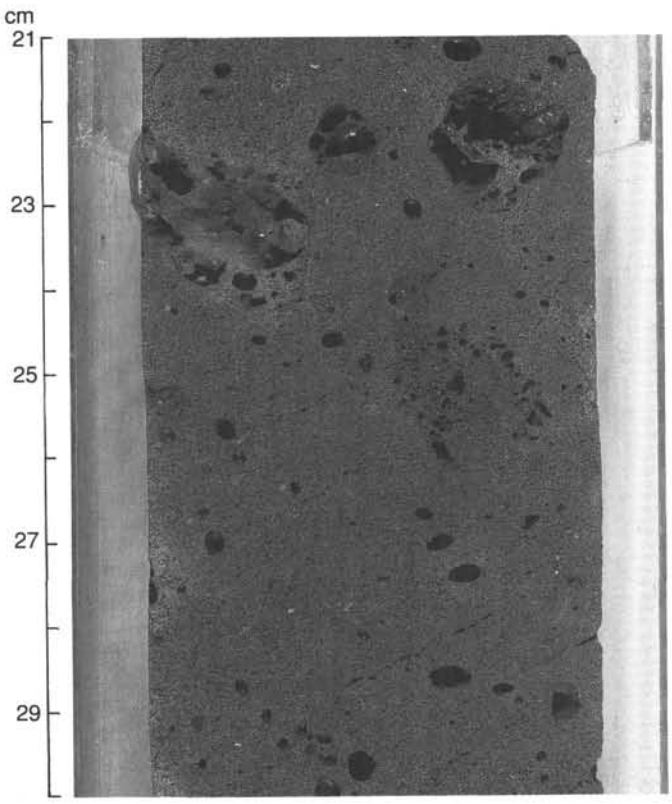

Figure 11. Close-up photo of a highly vesicular aphyric basalt flow (Interval 132-809F-2Z-1, 21–30 cm). Note the uniformly distributed submillimeter-scale vesicles common to all basalt samples from Hole 809F.

sequence is (1) cotectic crystallization of olivine, plagioclase, and clinopyroxene; (2) cotectic crystallization of plagioclase and clinopyroxene without olivine; (3) saturation or near saturation in titanomagnetite; (4) late crystallization of traces of ilmenite; and (5) sulfide segregation. An inference is that the basaltic liquids were initially undersaturated in sulfide, and only achieved saturation in the very latest stages of crystallization, following the joining of titanomagnetite to the crystallizing mineral assemblage.

Geochemistry

Eight samples were analyzed for major oxides and trace elements on board ship. Analytical conditions and are given in the "Explanatory Notes" chapter (this volume). Results are listed in Table 2. All analyzed samples are extremely fresh, containing no alteration minerals or stains observable in hand specimen. All have very low negative or even positive values for loss-on-ignition (LOI) in Table 2.

Four of the samples analyzed are ferrobasalts, the other four are olivine tholeiites. The four ferrobasalts are essentially identical in composition. Apart from one trace element, Ba, so also are the olivine tholeiites. On this basis, we distinguish the single sample analyzed from Core 132-809F-34B as a distinct chemical type.

Considering general geochemical attributes, the uppermost ferrobasalt and immediately underlying olivine tholeiite have the typical elevated K_2O (0.60% and 0.32%, respectively), Rb (10 and 5 ppm), and Ba (61 and 45 ppm) abundances, and the relatively low TiO_2 (1.7% at Mg# = 0.43; 1.2% at Mg# = 0.60), Zr (72 and 56 ppm) and Y (27 and 19 ppm) of many back-arc-basin basalts. They are virtually identical to basalts previously sampled

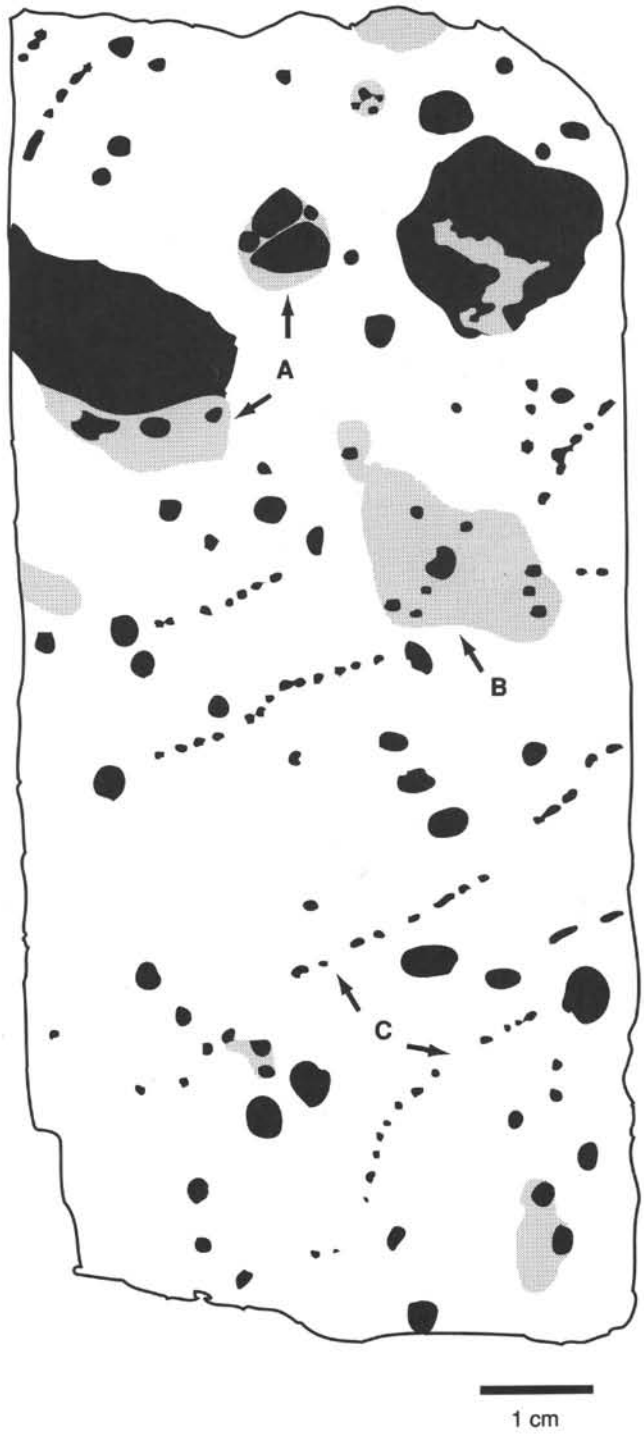

Figure 12. Line drawing of the photograph of Interval 132-809-2Z-1, 20–32 cm, in Figure 11. **A.** Segregation vesicles filled with vesiculated residual basalt. The glassy fill has collected at the floor of the vesicles. **B.** An inclusion of aphyric vesicular basalt. **C.** Sloping vesicle trails.

from this volcanic ridge (Hochstaedter et al., in press; Fryer et al., in press). They are also aluminous, having 1.5%–2% more Al_2O_3 contents than abyssal tholeiites at comparable Mg# (e.g., Fryer et al., 1982).

The lowermost basalt, obtained below the 50 m interval with no recovery, is similar to the olivine tholeiite above it, but it has somewhat lower K_2O contents (0.29% vs. 0.32%) and much lower

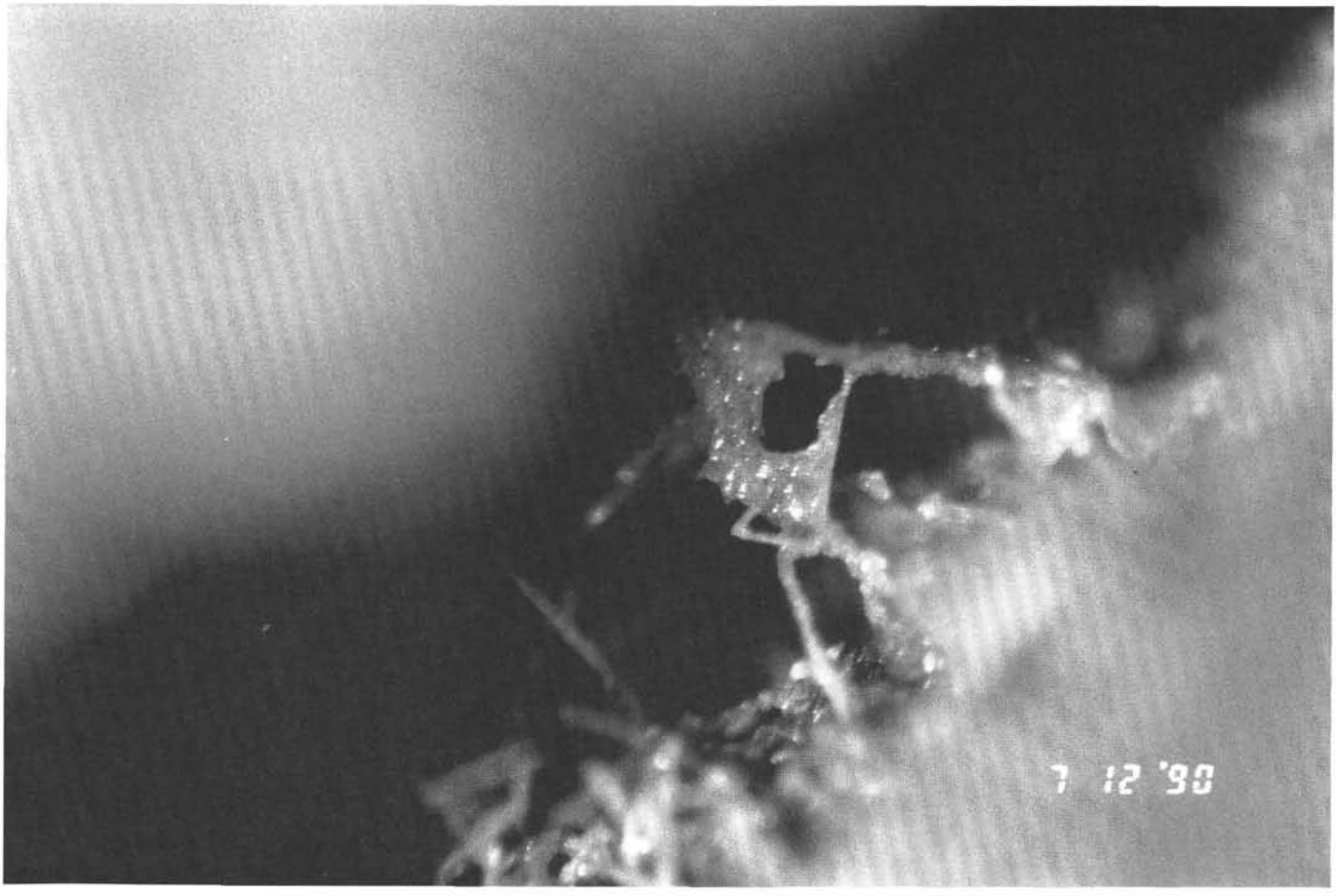

Figure 13. Photographic enlargement of a red, acicular, amygdule mineral. The needles are cemented by a clear translucent mineral. The vesicle is approximately 1.5 mm across (from Section 132-809F-11Z-2, about 23 cm; Piece 1B).

Ba (19 ppm). In these respects, it resembles basalts from Site 791 drilled just south of Central Ridge during Leg 126, which are interpreted to represented "syn-rift" basalts dating from the earliest stages of the opening of Sumisu Rift (Fujioka, Taylor, et al., 1989). The Ba contents of one small basalt chip recovered in Core 132-809F-22Z (one of the very few such in the interval of virtually no recovery) is 32 ppm, intermediate between the low value in the sample from Core 132-809F-34B, and that of the upper olivine tholeiites (45 ppm). Given the comparatively poor accuracy of Ba determinations by X-ray fluorescence (±10 ppm), the measurements will have to be made more precisely on shore, to establish the proper magnitude of these distinctions.

This last very subtle geochemical distinction allows us to speculate, albeit on meager evidence, that the interval of very low recovery represents highly vesicular and expanded basaltic glass, similar to that represented by the low-Ba rocks at Site 791. The rock compositions and stratigraphy suggest that we cored through a carapace of basalts similar to more typical back-arc-basin lavas, into possible "syn-rift" breccias deposited on subsided prerift basement, which projects on seismic profiler records to a shallow elevation at this location (G. Brown, pers. comm., 1990).

PALEOMAGNETICS

Introduction

The lack of an experienced paleomagnetist on Leg 132 prevented the detailed shipboard analysis of the magnetics data collected at Site 809. However, some discussion of the data is warranted. Volume magnetic susceptibility measurements of whole-core sections were taken at 15 cm intervals using the Bartington Magnetic Susceptibility Meter. Magnetic analyses were performed on the archive-half of the split core using the three-axis pass-through cryogenic rock magnetometer to obtain a record of natural remanent magnetization (NMR). The core sections were subjected to low-field, partial alternating-field (AF) demagnetization at levels of 5.0 and 10.0 mT, respectively. Significant amounts of scatter in the data resulted from the variable core recovery and the placement of plastic dividers in the coreliner between discrete rock pieces for archival purposes.

Magnetic Susceptibility

Volume magnetic susceptibility was measured on whole-core basaltic rocks recovered at Hole 809F when recovery allowed. The rocks were placed in split plastic coreliners and separated by plastic spacers before measurements were taken. The magnetic susceptibility data collected at Site 809 are presented in Table 3 and in Figure 16. Susceptibility averaged 1292 (10^{-6} cgs units) for all samples measured, however there are significant differences in the magnetic susceptibility of the rocks above and below 19.5 mbsf. This change in the amplitude of the susceptibility signal, illustrated in Figure 16, reflects a decrease in average volume magnetic susceptibility from 2308 (10^{-6} cgs units) in the upper zone to 512 (10^{-6} cgs units) below. Chemical analyses of the basalts indicate higher TiO_2 and Fe_2O_3 concentrations in the

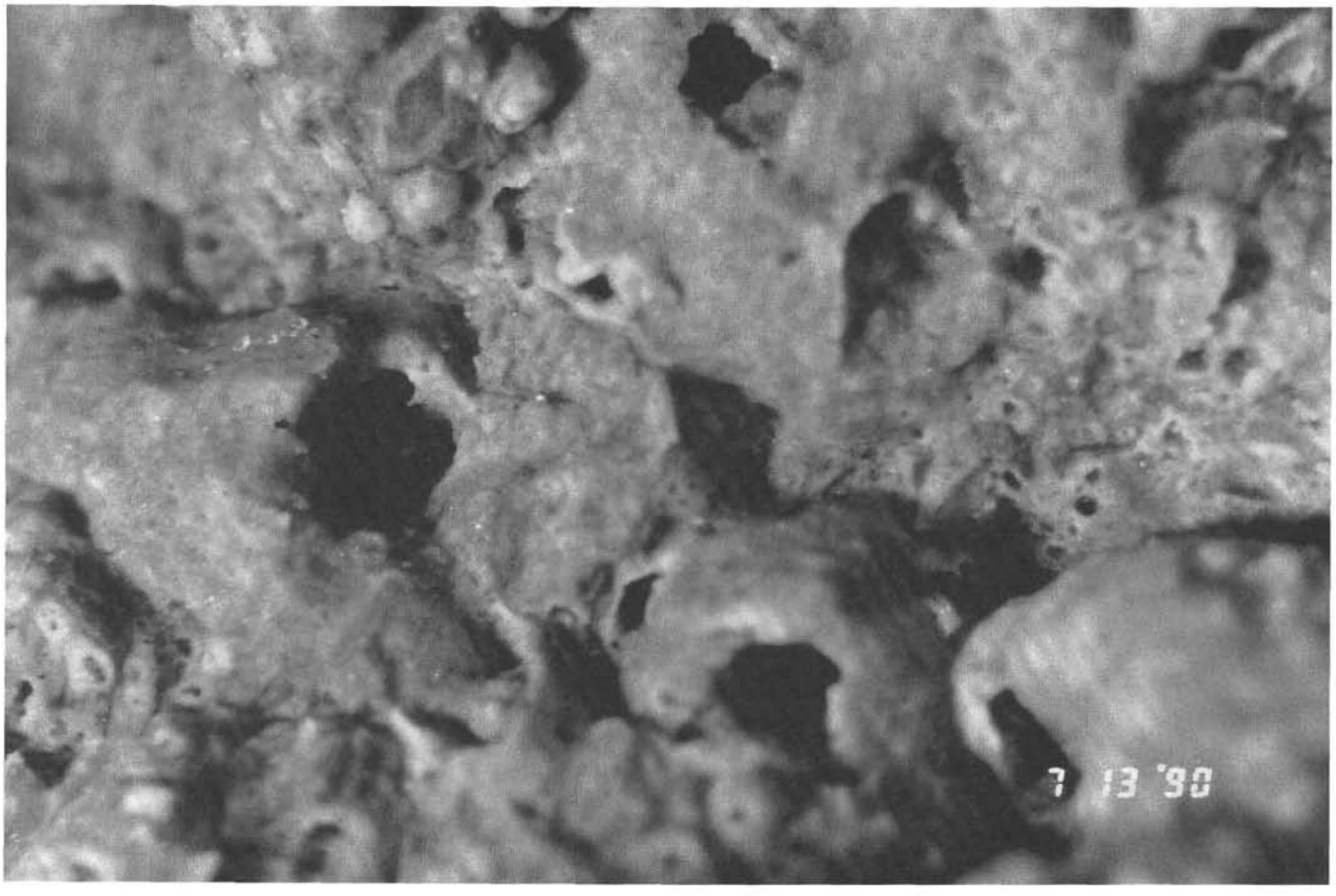

Figure 14. Bubbly precipitate on the wall of a cavity from Section 132-809F-17Z-1, about 8–10 cm (Piece 2). The field of view is approximately 2 mm across.

upper zone than in the lower zone. This corresponds to a greater abundance of titanomagnetite in the upper zone, which may account for its higher susceptibility.

Cryogenic Rock Magnetization

Natural remanent magnetization of the recovered basalts indicates that a possible magnetic shift from normal to reversed polarity occurs near 20.5 mbsf at the break between the upper ferrobasalt and the olivine tholeiite. This polarity reversal may correspond to the base of the Brunhes at 0.73 m.y.; although this identification is speculative. The declination, inclination, and intensity of the natural remanent magnetism (NMR) observed at Hole 809F are displayed in summary (Fig. 17. Alternating-field demagnetization (AFD) of the core sections resulted in the data displayed in Figure 18 at 5.0 mT AFD, and Figure 19 at 10.0 mT AFD. No discrete samples were measured from these cores during Leg 132. Samples for shorebased analysis using a spinner magnetometer should better define the nature of the magnetic record at this site.

PHYSICAL PROPERTIES

Introduction

A sequence of aphyric vesicular basalts was recovered at Site 809. Index properties (wet and dry bulk density, grain density, porosity, and water content) and compressional-wave velocity measurements were made on the recovered material. The compressional wave velocity data are listed in Table 4, and index-property data for these samples are presented in Tables 5 and 6.

Compressional Wave Velocity

The samples for compressional wave velocity measurements were taken from intact pieces of rock large enough for 1.5 to 1.8 cm long, 2.5 cm diameter minicores to be drilled into the split face of the core. Samples selected from each core were representative of the recovered units and variations in vesicularity downhole. The minicores were trimmed into cubic shapes with parallel faces using the double-bladed saw in the Core Lab. Velocities were measured at 500 kHz using the Hamilton Frame velocimeter after the samples were resaturated in filtered seawater for over 24 hr. The distance between sample faces, and thus the separation between the Hamilton Frame transducers, is measured using a micrometer whereas the traveltime of the 500 kHz pulse is measured using a pulse detector (see "Explanatory Notes" chapter, this volume).

Through a sampling oversight, the orientation of the minicores was only maintained with respect to the c-axis of the core, although measured velocities are reported for other relative orientations (see Table 4). However, these other orientations do give some idea as to the relative anisotropy in the rocks drilled.

The recovered sequence can be roughly divided at about 20 mbsf into high and low relative-velocity zones. In the upper cores the measured velocities averaged 4344 m/s along the c-axis (Fig. 20), 4364 m/s along the b-axis, and 4328 m/s along the a-axis (Fig. 21). Below 20 mbsf the measured average velocities decreased to 4036 m/s, 4076 m/s, and 4021 m/s for the c-, b-, and a-axes, respectively. The measured velocities increase again in Core 132-809F-17Z below about 27.0 mbsf to values comparable with

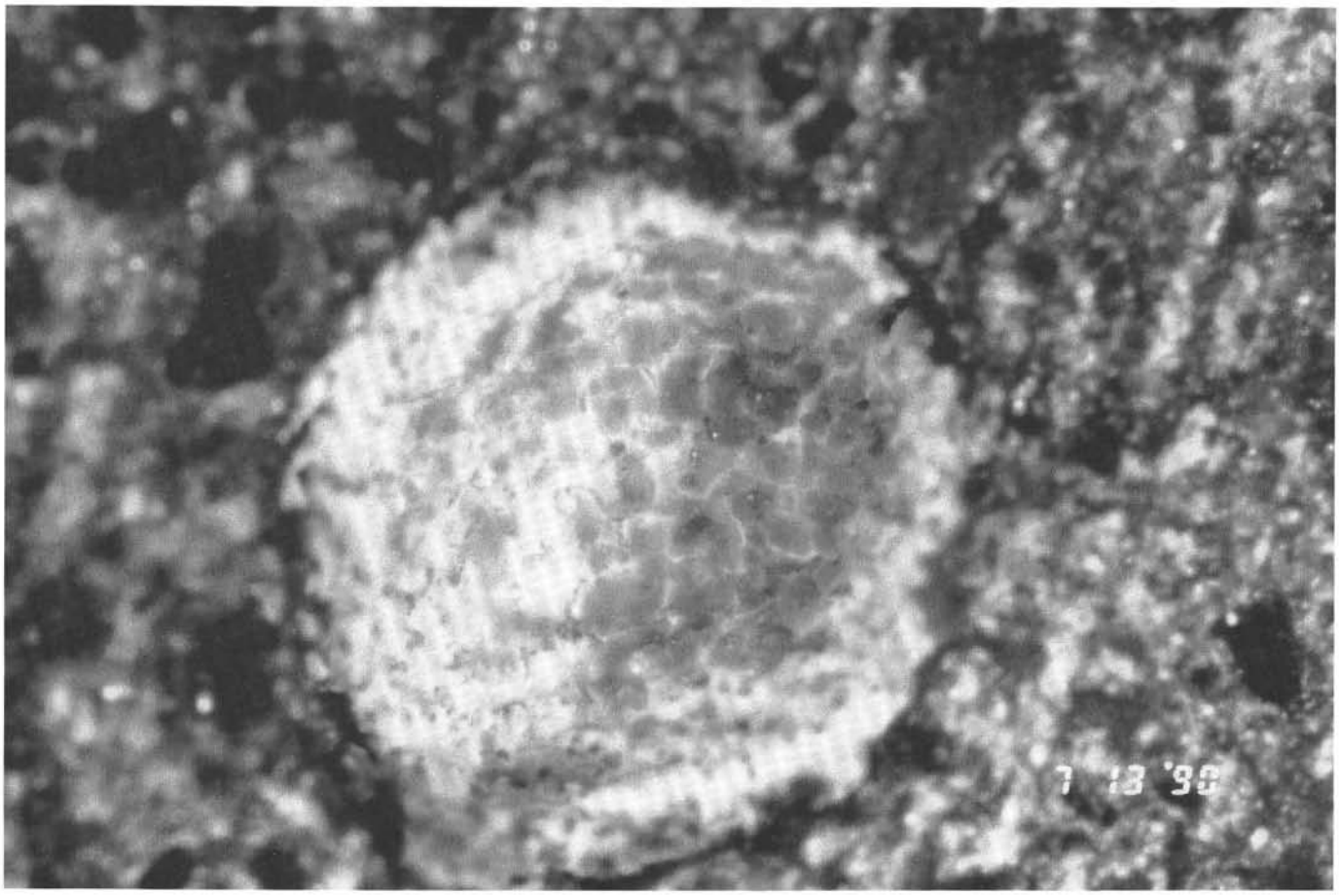

Figure 15. Yellow-green clays lining a small vesicle (1–2 mm across) in Section 132-809F-17Z-3, about 5 cm (Piece 1).

rocks from the upper zone. The differences in compressional velocities between the upper and lower zone is accounted for primarily by a 11% average increase in porosity in the deeper rocks (Fig. 22). This increase in average porosity is also evident in the average 0.2 g/cm^3 decrease in wet bulk density observed in the data (Fig. 23).

Index Properties

Index properties were measured on rock cubes after velocity determinations were made. The weight of each sample was determined using a Scientec electronic balance. Volume determinations were made using the Penta-pycnometer employing a 5.0 min purge with helium gas.

The distribution of physical properties measurements downhole is irregular and unevenly spaced because of variable core recovery; however some general trends are evident. Bulk densities are generally higher in the upper drilled sequence, averaging 2.66 and 2.43 g/cm^3 for wet and dry bulk density respectively. The measured values decrease below 20 mbsf to 2.46 and 2.12 g/cm^3 for wet and dry average bulk density, respectively. Grain density is approximately the same for the 19 samples tested, averaging 3.00 g/cm^3 (see Fig. 23), indicating that differences in bulk density are primarily attributable to porosity changes in the rocks. Duplicate determinations were conducted on each sample with errors of 1%–3%. Slightly lower grain densities in the upper zone may indicate a different mineralogy for the shallow rock samples. Chemical analyses of the basalts indicate slightly different concentrations of oxides between the upper and lower basalt types. MgO and CaO concentrations are higher in the deeper basalts relative to the shallower rocks whereas Fe_2O_3 and K_2O concentrations are lower.

Gravimetric determinations of porosity indicate an increase in average porosity from 22% in the upper zone to 33% in the lower sequence. Void ratio—the ratio of the volume of the voids to the volume of the solids in a sample—follow the trends observed in porosity (Fig. 24).

Decreased bulk densities and increased porosities are associated with the vesicular basalts found in samples from Cores 132-809F-13Z to 132-809F-17Z. Samples 132-809F-13Z-1, 54–56 cm, 132-17Z-3, 5–7 cm, and 132-17Z-2, 57–59 cm, are exceptions which have velocity-density values more like those from Cores 132-809F-11Z and 132-809F-2Z. The highest densities and lowest porosities for the hole were measured on Sample 132-809F-10Z-1, 7–8 cm. This sample had wet-bulk and dry-bulk densities of 2.78 and 2.61 g/cm^3, respectively, and a porosity of about 16%. The grain densities calculated for the 19 samples tested ranged from 2.94 to 3.04 g/cm^3.

Discussion and Conclusions

The velocity-density relationships at Hole 809F are illustrated in Figure 25. The compressional wave velocities measured along each axis generally increase with increasing wet bulk density as one would expect. The velocity and density patterns are controlled by the vesicularity of the basalts as seen in the porosity data. The lack of recovery in the deeper part of the hole prevented sampling below about 28 mbsf at this site.

Table 2. Shipboard XRF analyses of basalts from Hole 809F (D. Sims, analyst).

	Type I			Type II				Type III
Section 1	809F-2Z-1	809F-8Z-1	809F-11Z-2	809F-14Z-1	809F-16Z-1	809F-17Z-2	809F-22Z-	809F-34B-1
Interval (cm)	20–24	2–4	50–53	6–10	39–42	31–36	5–7	10–15
SiO_2	50.11	50.41	50.57	48.79	50.16	49.65	49.71	48.92
TiO_2	1.70	1.69	1.72	1.21	1.28	1.24	1.22	1.21
Al_2O_3	15.93	15.73	15.85	16.72	16.20	16.39	16.36	16.55
Fe_2O_3 (T)	13.81	13.76	13.75	10.58	11.69	10.87	11.03	11.04
MnO	0.22	0.22	0.23	0.17	0.19	0.18	0.18	0.18
MgO	4.56	4.61	4.60	6.86	7.01	6.95	7.01	7.16
CaO	9.70	9.59	9.65	12.60	12.51	12.53	12.55	12.58
Na_2O	2.98	3.05	2.98	2.18	2.22	2.27	2.17	2.24
K_2O	0.54	0.60	0.53	0.32	0.36	0.33	0.34	0.29
P_2O_5	0.27	0.26	0.27	0.16	0.15	0.15	0.15	0.15
—	99.82	99.92	100.15	99.59	101.77	100.56	100.72	100.32
Trace elements (ppm)								
Ba	55	51	61	45	65	56	33	19
Rb	8	10	8	6	6	5	5	5
Nb	1.3	1.2	0.9	1.3	1.2	1.2	1.4	.0
Ce	12	10	12	6	12	10	9	12
Zr	71	73	72	56	59	57	57	55
Sr	283	281	283	243	246	240	240	247
Y	26	26	27	19	21	20	20	20
Cu	49	49	48	82	87	82	83	85
Zn	87	82	91	59	62	58	57	54
V	444	423	453	355	372	361	358	351
Ni	8	8	7	55	48	48	51	48
Cr	2	2	2	172	136	151	157	145
LOI	−0.16	−0.33	−0.12	−0.00	−0.02	−0.11	−0.11	+0.23
[a]Mg#	0.432	0.436	0.435	0.599	0.580	0.596	0.594	0.599

[a] Computed assuming $Fe^{2+}/(Fe^{2+} + Fe^{3+}) = 0.86$.

The grain density values at Hole 809F compare favorably with data from rocks drilled at Site 648 during ODP Legs 106 and 109. The compressional velocities and bulk densities from Hole 809F are much lower than those reported from the Mid-Atlantic Ridge, however the Site 809 basalts have higher porosity than the average of 4.5% at Site 648. The high degree of vesicularity in the young basaltic rocks at Site 809 probably accounts for most of these differences, although grain size variations and microstructural differences may also contribute to changes in the velocity-density relationships. Carlson and Wilkens (1983) discuss density and velocity values for laboratory studies on rocks from the West Philippine Basin that are similar to the values measured at Site 809.

The high porosities, low densities, and slow velocities of the basalts drilled in the Sumisu Rift are in sharp contrast to the much lower porosities and higher velocities measured in the laboratory on basalts from the East Pacific Rise (Warren and Rosendahl, 1980).

REFERENCES

Brown, G., and Taylor, B., 1988. Sea-floor mapping of the Sumisu Rift, Izu-Ogasawara (Bonin) island arc. *Chishitsu Chosasho Geppo,* 39:23–38.

Carlson, R. L., and Wilkens, R. H. 1983. Seismic crustal structure and the elastic properties of rocks recovered by drilling in the Philippine Sea. *In* Hilde, T.W.C., and Uyeda, S. (Eds.), *Geodynamics of the Western Pacific-Indonesian Region:* Am. Geophys. Union, AGU Geodynamics Ser., 11:127–136.

Dick, H.J.B., 1980. Vesicularity of Shikoku Basin basalt, Deep Sea Drilling Project, Leg 58. *In* Klein, G., Kobayashi, K., et al., *Init. Repts. DSDP,* 58: Washington (U.S. Govt. Printing Office), 895–901.

Fryer, P., Langmuir, C. H., Hochstaedter, A. G., and Taylor, B., in press. Petrology and geochemistry of igneous dredge samples from the Sumisu backarc rifts. *Earth Planet. Sci. Lett.*

Fryer, P., Sinton, J. N., and Philpotts, J. A., 1982. Basaltic glasses from the Mariana Trough. *In* Hussong, D. M., Uyeda, S., et al., *Init. Repts. DSDP,* 60: Washington (U.S. Govt. Printing Office), 601–609.

Fujioka, K, Taylor, B., et al., 1989. Arc volcanism and rifting. *Nature,* 342:1819.

Garcia, M. O., Liu, N.W.K., and Muenow, D. W., 1979. Volatiles in submarine volcanic rocks from the Mariana island arc and trough. *Geochim. Cosmochim. Acta,* 43:305–312.

Hochstaedter, A. G., Gill, J. B., Langmuir, C. H., Morris, J. D., and Pringle, M., in press. Petrology and geochemistry of lavas from the Sumisu Rift: An incipient back-arc basin. *Earth Planet. Sci. Lett.*

Honza, E., and Tamaki, T., 1985. Bonin Arc. *In* Nairn, A.E.M., and Uyeda, S. (eds.), *The Ocean Basins and Margins,* 7: The Pacific Ocean: New York (Plenum Press), 459–502.

Hussong, D. M., and Uyeda, S., 1982. Tectonic processes and the history of the Mariana arc: A synthesis of the results of Deep Sea Drilling Project Leg 60. *In* Hussong, D. M., Uyeda, S., et al., *Init. Repts. DSDP,* 60: Washington (U.S. Govt. Printing Office), 909–929.

Sato, H., 1979. Segregation vesicles and immiscible liquid droplets in ocean-floor basalt of Hole 396B, DSDP Leg 46. *In* Dmitriev, L., Heirtzler, J., et al., *Init. Repts. DSDP,* 46: Washington (U.S. Govt. Printing Office), 283–291.

Smith, J. R., Taylor, B., Malahoff, A., and Peterson, L., in press. Submersible and deep-tow camera studies of submarine volcanic terrains in the Sumisu Rift, Izu-Bonin arc. *Earth Planet. Sci. Lett.*

Smith, R. E., 1968. Segregation vesicles in basaltic lava, *Am. J. Sci.,* 265: 696–713.

Taylor, B., Brown, G., Fryer, P., and Hussong, D., in press. Rifting of the Bonin island arc. *J. Geophys. Res.*

Urabe, T., and Kusakabe, M., in press. Barite-silica chimneys from the Sumisu Rift, Bonin (Izu-Ogasawara) arc: Product of Kuroko-type hydrothermal mineralization. *Earth Planet. Sci. Lett.*

Warren, N., and Rosendahl, B. R., 1980. Velocity-density systematics for basalts drilled on the East Pacific Rise and Galapagos Rift during Deep Sea Drilling Project Leg 54. *In* Rosendahl, B. R., Kekinian, R., et al.., *Init. Repts. DSDP,* 54: Washington (U.S. Govt. Printing Office), 853–863.

Ms 132A-103

NOTE: All core description forms ("barrel sheets") and core photographs have been printed on coated paper and bound as Section 4, near the back of the book, beginning on page 241.

Table 3. Magnetic susceptibility data of basalts from Hole 809F.

Core, section	Interval (cm)	Depth (mbsf)	Magnetic susceptibility
1Z-1	4.5	5.95	110
1Z-1	14.5	6.05	264
2Z-1	4.5	6.24	1275
2Z-1	14.5	6.34	1387
2Z-1	24.5	6.44	2263
2Z-1	34.5	6.54	2280
2Z-1	44.5	6.64	2451
2Z-1	54.5	6.74	1451
2Z-1	64.5	6.84	624
2Z-1	74.5	6.94	143
2Z-2	4.5	7.03	2240
8Z-1	4.5	13.94	3254
9Z-1	4.5	14.05	2953
10Z-1	4.5	14.44	3286
11Z-1	4.5	14.65	2728
11Z-1	14.5	14.75	3112
11Z-1	24.5	14.85	3080
11Z-1	34.5	14.95	3217
11Z-1	44.5	15.05	4034
11Z-1	54.5	15.15	4073
11Z-2	4.5	15.30	3575
11Z-2	14.5	15.40	4036
11Z-2	24.5	15.49	3901
11Z-2	34.5	15.60	3758
11Z-2	44.5	15.69	3648
11Z-2	54.5	15.80	3715
11Z-2	64.5	15.90	3458
11Z-3	4.5	16.05	1230
11Z-3	14.5	16.15	3359
11Z-3	24.5	16.25	3400
11Z-3	34.5	16.34	3142
11Z-3	44.5	16.44	2357
13Z-1	4.5	19.44	676
13Z-1	14.5	19.55	633
13Z-1	24.5	19.65	265
13Z-1	34.5	19.74	471
13Z-1	44.5	19.84	968
13Z-1	54.5	19.94	893
13Z-1	64.5	20.05	159
13Z-1	74.5	20.15	181
13Z-2	4.5	20.19	508
13Z-2	14.5	20.30	267
13Z-2	24.5	20.40	440
14Z-1	4.5	20.55	544

Table 3 (continued).

Core, section	Interval (cm)	Depth (mbsf)	Magnetic susceptibility
14Z-1	14.5	20.65	508
14Z-1	24.5	20.75	428
14Z-1	34.5	20.84	223
14Z-1	44.5	20.94	343
14Z-1	54.5	21.05	333
14Z-1	64.5	21.15	370
14Z-1	74.5	21.25	62
14Z-2	4.5	21.30	373
14Z-2	14.5	21.40	243
14Z-2	24.5	21.50	317
14Z-2	34.5	21.59	319
14Z-2	44.5	21.69	335
14Z-2	54.5	21.80	862
14Z-2	74.5	22.00	235
14Z-3	4.5	22.05	838
14Z-3	4.5	22.05	336
14Z-3	14.5	22.15	968
14Z-3	14.5	22.15	363
14Z-3	24.5	22.25	981
14Z-3	24.5	22.25	990
14Z-3	34.5	22.34	313
14Z-3	34.5	22.34	1129
14Z-3	44.5	22.44	260
14Z-3	44.5	22.44	519
14Z-3	54.5	22.55	560
14Z-3	54.5	22.55	259
14Z-3	64.5	22.65	614
14Z-3	64.5	22.65	801
14Z-3	74.5	22.75	355
14Z-3	74.5	22.75	8
17Z-2	4.5	27.05	1129
17Z-2	14.5	27.15	858
17Z-2	24.5	27.25	469
17Z-2	34.5	27.34	876
17Z-2	44.5	27.44	787
17Z-2	54.5	27.55	521
17Z-2	64.5	27.65	536
17Z-3	4.5	27.69	802
17Z-3	14.5	27.80	833
17Z-3	24.5	27.90	264
18Z-1	14.5	29.45	163
19Z-1	14.5	32.45	304
20Z-1	14.5	35.45	1478

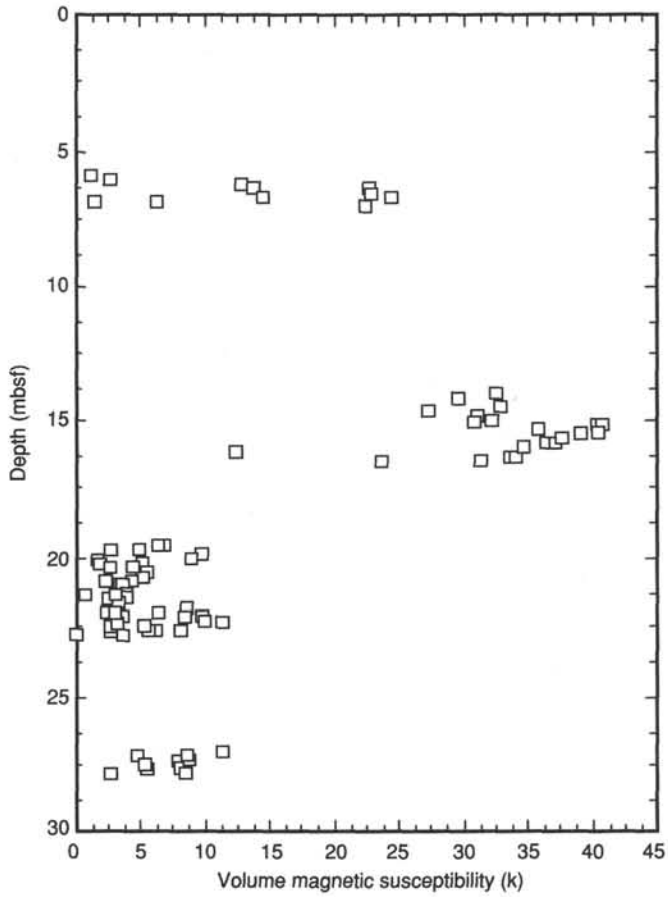

Figure 16. Plot of magnetic susceptibility data in Table 3.

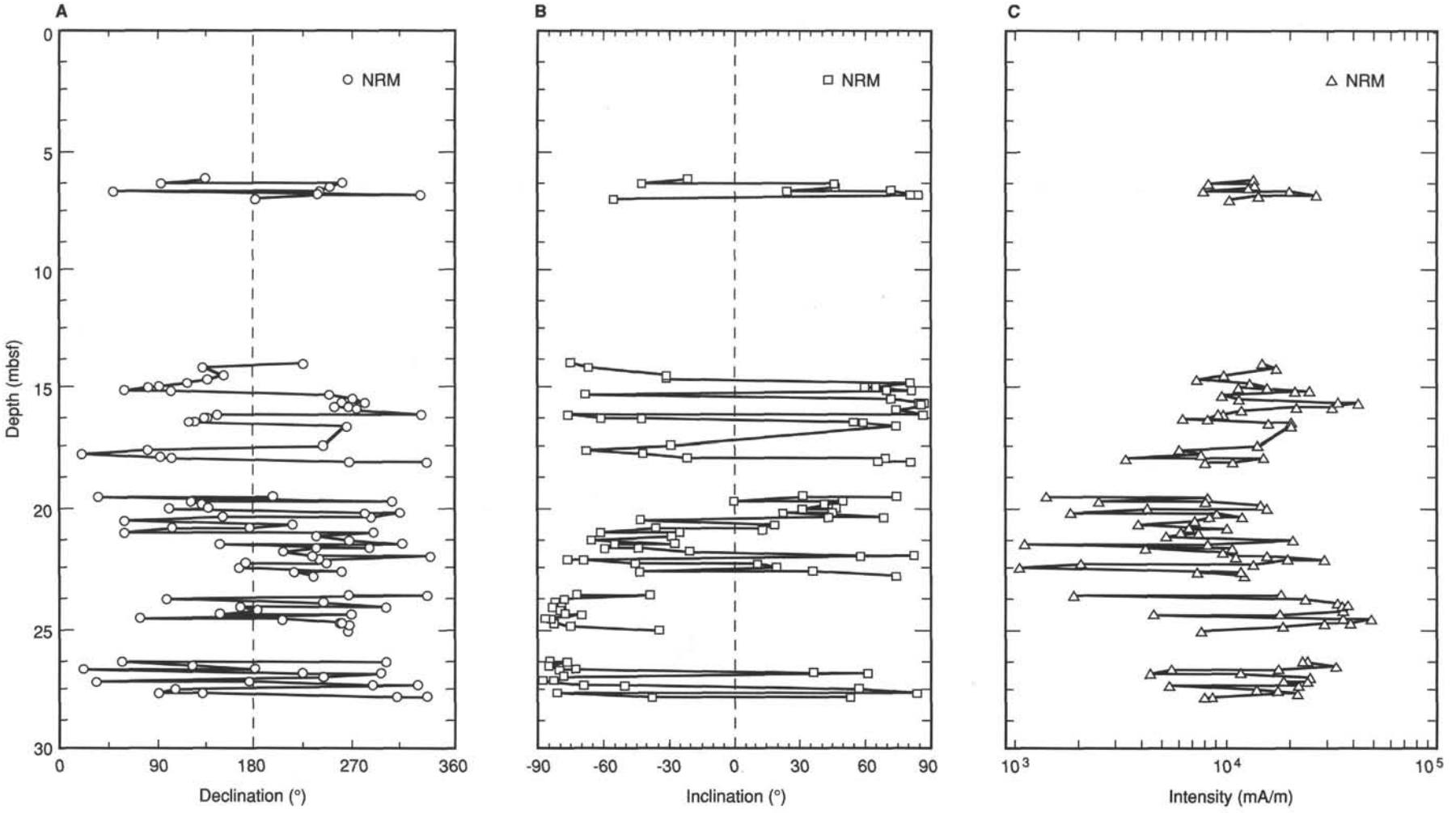

Figure 17. Plot of natural remanent magnetization of basalts from Hole 809F. **A.** Declination. **B.** Inclination. **C.** Intensity.

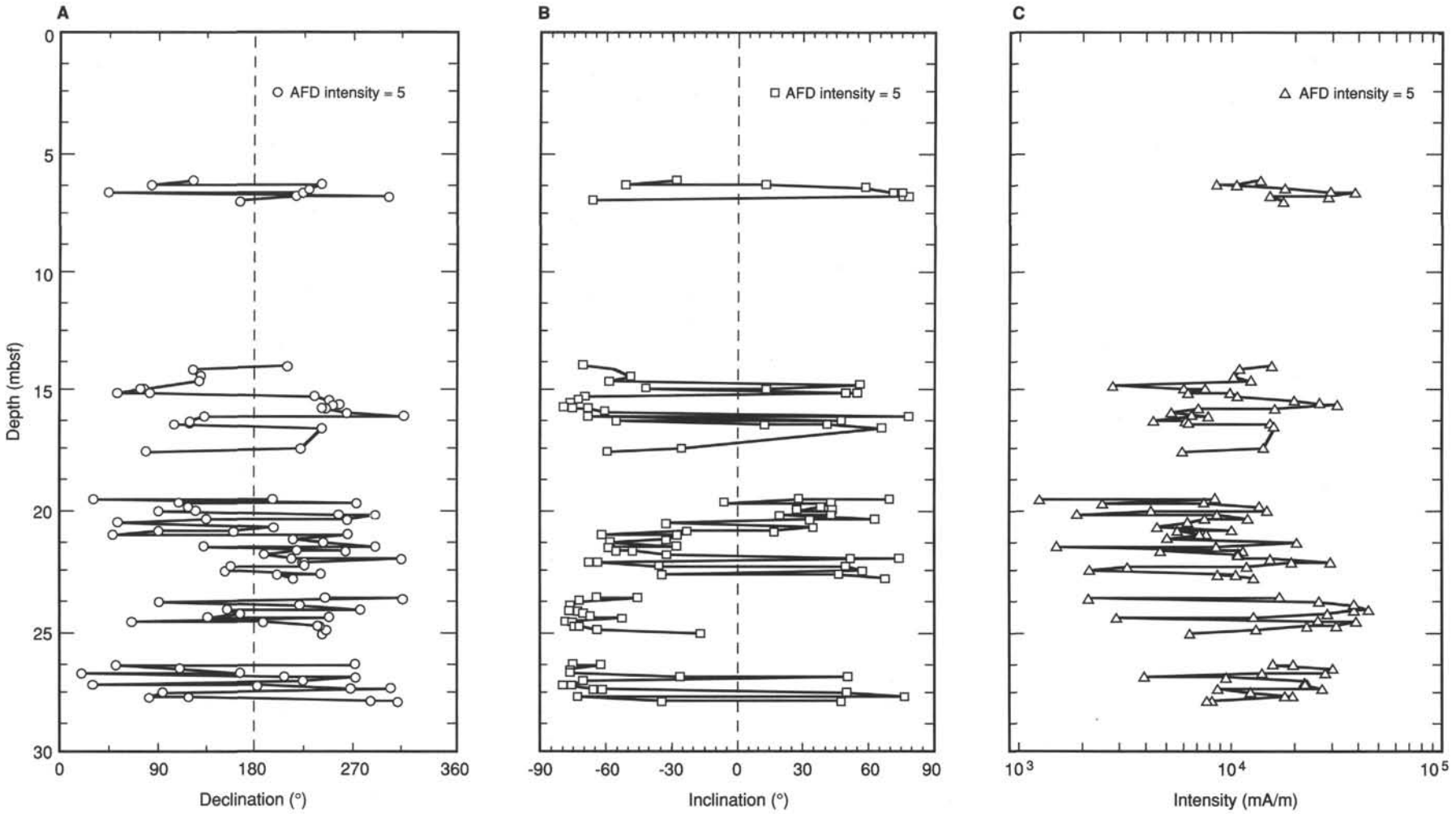

Figure 18. Plot of alternating field demagnetization at 5.0 mT of basalts from Hole 809F. **A.** Declination. **B.** Inclination. **C.** Intensity.

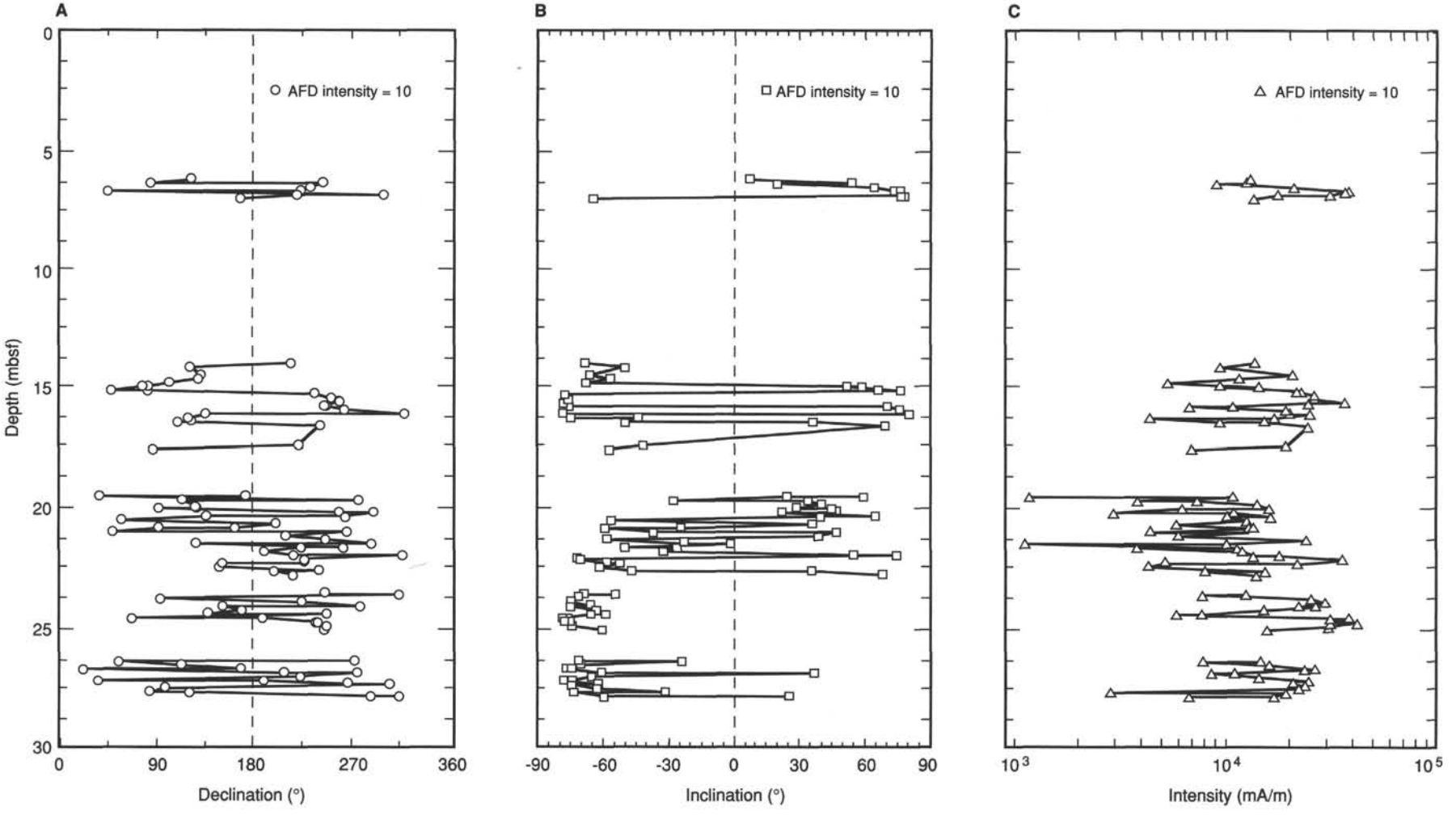

Figure 19. Plot of alternating field demagnetization at 10.0 mT of basalts from Hole 809F. **A.** Declination. **B.** Inclination. **C.** Intensity.

Table 4. Compressional wave velocities measured at Hole 809F using the Hamilton Frame velocimeter. D = direction of measurement relative to the axis of the split core.

Core, section, interval (cm)	Depth (mbsf)	D	Velocity C (km/s)	D	Velocity B (km/s)	A	Velocity A (km/s)
2Z-1, 24—25	6.44	[a]C	4.878	[a]B	4.751	[a]A	4.764
2Z-1, 24—25	6.44	C	4.893	B	4.693	A	4.754
10Z-1, 7—8	14.47	C	4.150	B	4.293	A	4.287
10Z-1, 7—8	14.47	C	4.118	B	4.335	A	4.234
11Z-1, 7—8	14.67	C	4.457	B	4.497	A	4.472
11Z-1, 7—8	14.67	C	4.433	B	4.523	A	4.472
11Z-2, 34—35	15.59	C	4.610	B	4.495	A	4.452
11Z-2, 34—35	15.59	C	4.543	B	4.498	A	4.444
11Z-2, 48—50	15.73	C	4.308	B	4.290	A	4.381
11Z-2, 48—50	15.73	C	4.394	B	4.352	A	4.363
11Z-3, 11—13	16.11	C	4.229	B	4.332	A	4.288
11Z-3, 11—13	16.11	C	4.250	B	4.304	A	4.280
11Z-3, 36—38	16.36	C	4.148	B	4.166	A	4.000
11Z-3, 36—38	16.36	C	4.143	B	4.153	A	3.989
13Z-1, 40—42	19.80	C	3.839	B	3.816	A	3.838
13Z-1, 40—42	19.80	C	3.826	B	3.791	A	3.910
13Z-1, 54—56	19.94	C	4.496	B	4.607	A	4.499
13Z-1, 54—56	19.94	C	4.478	B	4.657	A	4.481
14Z-1, 15—17	20.65	C	3.918	B	3.758	A	3.854
14Z-1, 15—17	20.65	C	3.888	B	3.664	A	3.834
14Z-1, 41—42	20.91	C	4.139	B	4.307	A	4.071
14Z-1, 41—42	20.91	C	4.150	B	4.219	A	4.032
14Z-2, 61—63	21.86	C	3.897	B	3.886	A	3.907
14Z-2, 61—63	21.86	C	3.840	B	3.885	A	3.895
14Z-3, 22—24	22.22	C	3.777	B	3.914	A	3.932
14Z-3, 22—24	22.22	C	3.803	B	3.905	A	3.921
16Z-1, 56—58	24.36	C	4.144	B	4.166	A	4.170
16Z-1, 56—58	24.36	C	4.170	B	4.149	A	4.204
16Z-2, 19—21	24.66	C	3.960	B	3.960	A	3.969
16Z-2, 19—21	24.66	C	3.964	B	3.946	A	4.010
17Z-1, 33—35	26.63	C	3.812	B	3.895	A	3.847
17Z-1, 33—35	26.63	C	3.807	B	3.914	A	3.800
17Z-2, 4—6	27.04	C	3.811	B	3.829	A	3.639
17Z-2, 4—6	27.04	C	3.828	B	3.830	A	3.661
17Z-2, 57—59	27.57	C	4.602	B	4.734	A	4.552
17Z-2, 57—59	27.57	C	4.587	B	4.732	A	4.525
17Z-3, 5—7	27.70	C	4.315	B	4.412	A	4.278
17Z-3, 5—7	27.70	C	4.306	B	4.419	A	4.327

[a] C = velocity along vertical axis. A, B = velocities along orthogonal axes perpendicular to C.

Table 5. Bulk and grain densities[a] determined gravimetrically using the Penta pycnometer at Hole 809F.

Core, section, interval (cm)	Depth (mbsf)	WBD (g/cm^3)	DBD (g/cm^3)	GD (g/cm^3)
2Z-1, 24—25	6.44	2.63	2.40	2.94
10Z-1, 7—8	14.47	2.78	2.61	2.98
11Z-1, 7—8	14.67	2.71	2.53	2.96
11Z-2, 34—35	15.59	2.70	2.49	2.95
11Z-2, 48—50	15.73	2.68	2.46	2.96
11Z-3, 11—13	16.11	2.62	2.39	3.01
11Z-3, 36—38	16.36	2.59	2.34	3.02
13Z-1, 40—42	19.80	2.45	2.10	3.00
13Z-1, 54—56	19.94	2.71	2.51	3.00
14Z-1, 15—17	20.65	2.38	2.01	3.02
14Z-1, 41—42	20.91	2.47	2.12	2.99
14Z-2, 61—63	21.86	2.38	2.02	3.02
14Z-3, 22—24	22.22	2.47	2.13	3.00
16Z-1, 56—58	24.36	2.42	2.06	2.98
16Z-2, 19—21	24.66	2.43	2.07	2.98
17Z-1, 33—35	26.63	2.43	2.08	3.04
17Z-2, 4—6	27.04	2.45	2.12	3.04
17Z-2, 57—59	27.57	2.57	2.31	3.03
17Z-3, 5—7	27.7	2.57	2.27	3.00

[a]WBD = wet bulk density. DBD = dry bulk density. GD = grain density.

Table 6. Porosity, water content, and void ratios determined gravimetrically using the Penta pycnometer at Hole 809F.[a]

Core, section, interval (cm)	Depth (mbsf)	Por1 (%)	Por2 (%)	WWC (%)	DWC (%)	VR1 (e)	VR2 (e)
2Z-1, 24—25	6.44	22.1	21.4	8.6	9.4	0.28	0.27
10Z-1, 7—8	14.47	16.1	15.7	6.0	6.3	0.19	0.18
11Z-1, 7—8	14.67	17.3	16.9	6.5	7.0	0.21	0.20
11Z-2, 34—35	15.59	20.7	19.8	7.8	8.5	0.26	0.24
11Z-2, 48—50	15.73	21.8	20.9	8.3	9.1	0.28	0.26
11Z-3, 11—13	16.11	22.4	22.1	8.7	9.6	0.29	0.28
11Z-3, 36—38	16.36	24.4	24.1	9.7	10.7	0.32	0.32
13Z-1, 40—42	19.80	33.5	32.5	14.0	16.3	0.50	0.48
13Z-1, 54—56	19.94	19.8	19.3	7.5	8.1	0.25	0.24
14Z-1, 15—17	20.65	36.2	35.4	15.6	18.4	0.57	0.54
14Z-1, 41—42	20.91	34.3	32.8	14.2	16.6	0.52	0.48
14Z-2, 61—63	21.86	35.0	34.5	15.0	17.7	0.54	0.52
14Z-3, 22—24	22.22	32.4	31.5	13.5	15.6	0.48	0.46
16Z-1, 56—58	24.36	34.8	33.6	14.7	17.3	0.53	0.50
16Z-2, 19—21	24.66	34.7	33.5	14.7	17.2	0.53	0.50
17Z-1, 33—35	26.63	34.1	33.5	14.4	16.8	0.52	0.50
17Z-2, 4—6	27.04	31.7	31.3	13.3	15.3	0.46	0.45
17Z-2, 57—59	27.57	25.9	25.6	10.3	11.5	0.35	0.34
17Z-3, 5—7	27.7	28.8	27.7	11.5	13.0	0.40	0.38

[a] Por = porosity; WWC = wet water content; DWC = dry water content; VR = void ratio.

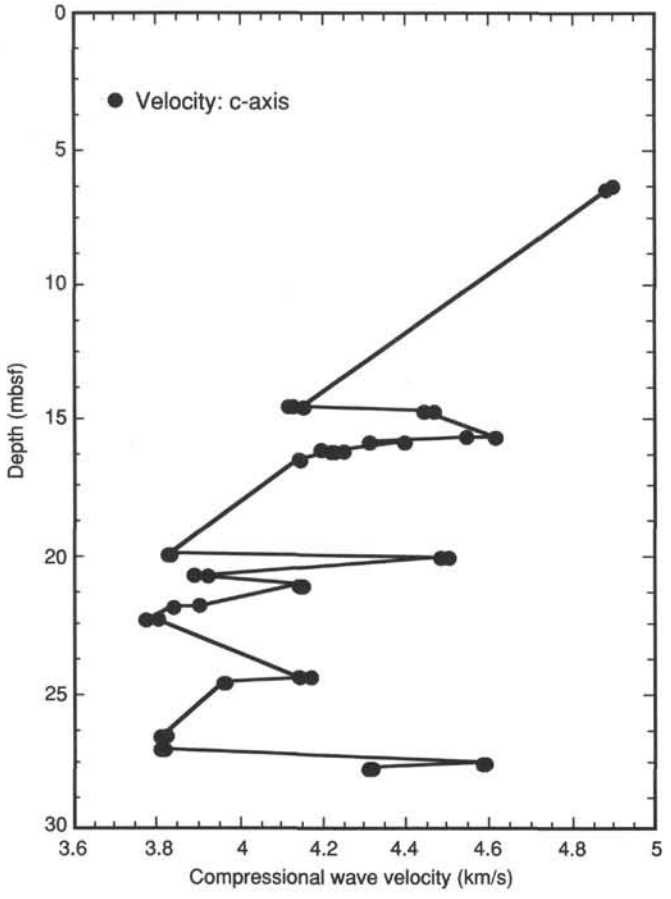

Figure 20. Compressional wave velocity measured along the c-axis of the core vs. depth at Hole 809F.

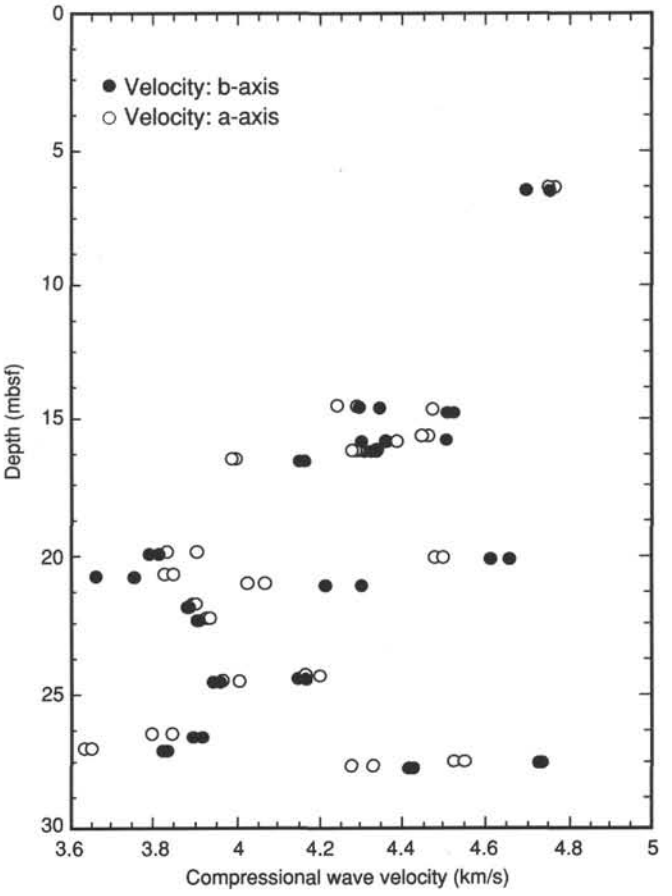

Figure 21. Compressional wave velocity measured along the b- and a-axes of the core vs. depth at Hole 809F.

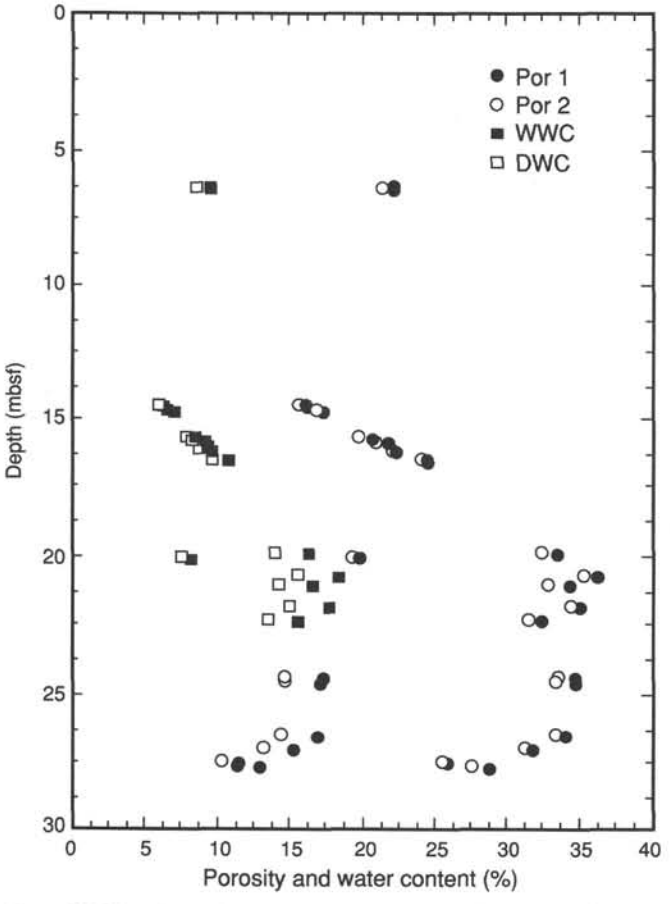

Figure 22. Plot of porosity and water content vs. depth at Hole 809F. Por1 and Por2 are calculated using the wet volume and dry volume of sample, respectively. WWC = wet water content; DWC = dry water content.

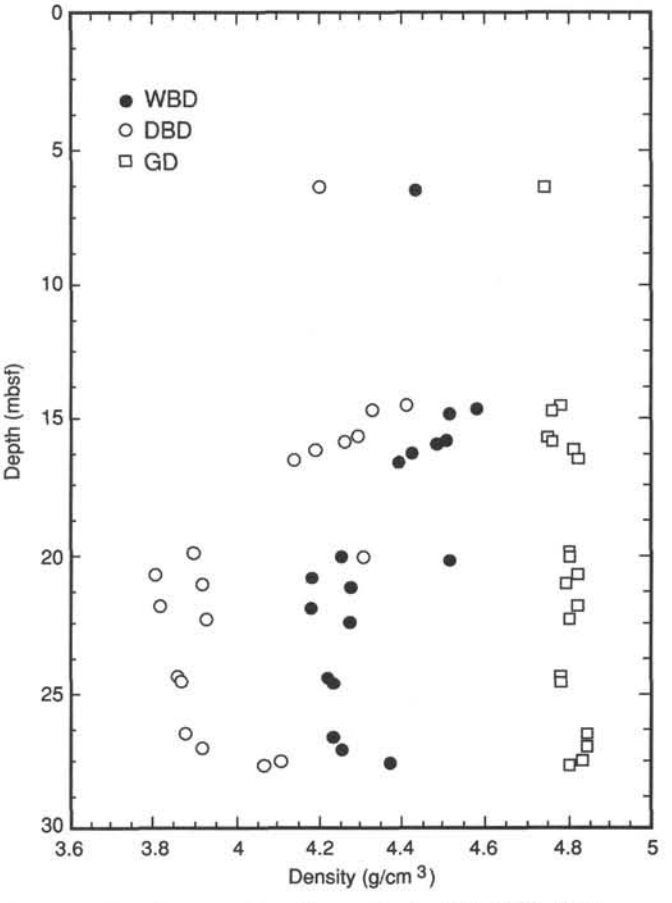

Figure 23. Plot of measured densities vs. depth at Hole 809F. WBD = wet bulk density; DBD = dry bulk density; GD = grain density.

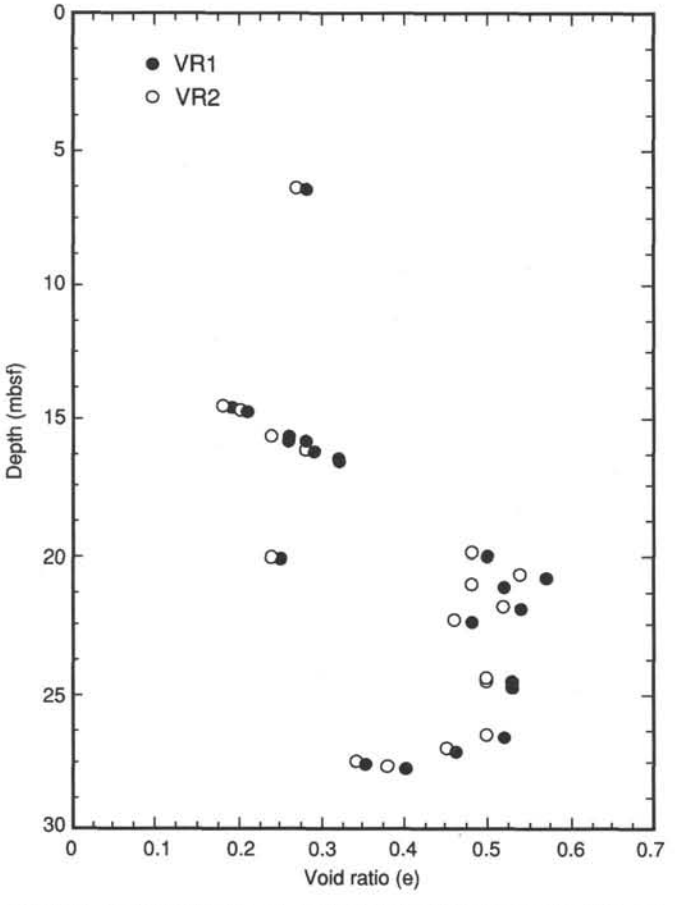

Figure 24. Plot of void ratio vs. depth at Hole 809F. Void ratios VR1 and VR2 are calculated using wet volume and dry volume of sample, respectively.

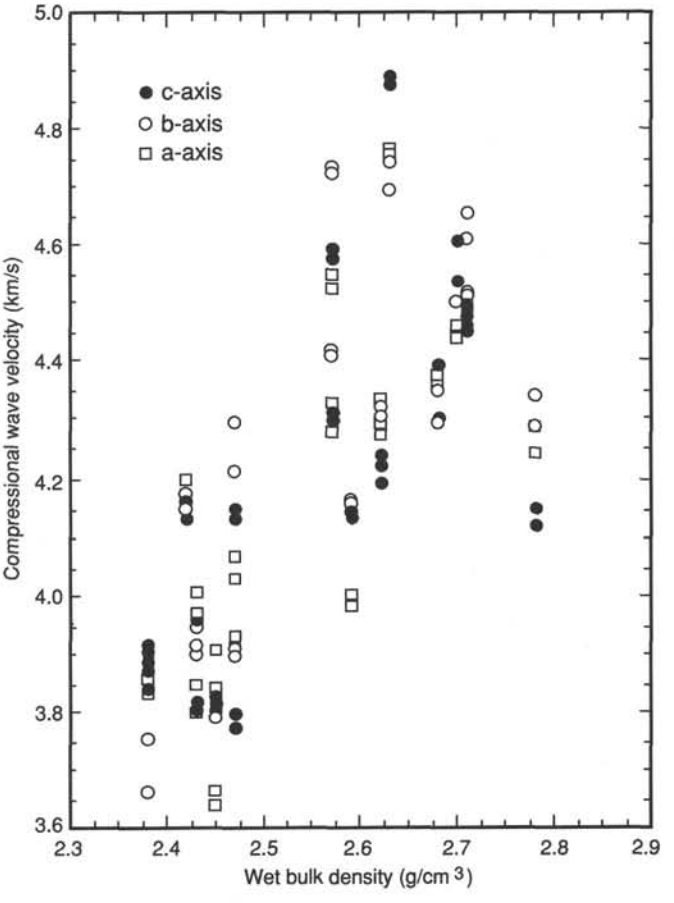

Figure 25. Summary of compressional wave velocities vs. wet bulk densities for all samples at Hole 809F.